Author's response by Daocheng Gong et al.

Corresponding to: tbongue@jnu.edu.cn

We greatly appreciate the time and effort that the Referees spent in reviewing our manuscript. The comments are really thoughtful and helpful to improve the quality of our paper. We have addressed each comment below, with the Referee comment in **black** text, our response in **blue** text, and relevant manuscript changes noted in **red** text. In addition, the readability of this manuscript has been improved by slightly changing the structure and polishing the language. The revised manuscript with relevant changes marked up has been attached to the end of our responses.

Comments by Referee #2:

The authors present field measurements of isoprene, MACR and MVK at a forested mountain site in southern China. Relatively lower concentration levels of isoprene and higher ratios of (MVK+MACR)/isoprene than other forest sites were observed. The authors argued that the low isoprene levels were ascribed to the strong atmospheric oxidative capacity in the region, and a chemical box model constrained with observations further confirmed this argument. Overall, this paper presents new data of isoprene and its first-stage degradation intermediates in a unique environment with interactions of both biogenic and anthropogenic emissions. It is well organized and written. Therefore, this manuscript can be considered for publication after the following specific comments being properly addressed.

Response: We thank the referee for this overview. We have made changes to the manuscript based on the referee's helpful comments.

The authors used an MCM chemical box model to predict the concentrations of OH and NO$_3$ radicals. This model has been applied in several previous studies. However, there are still several issues that

need to be clarified, and some additional modeling runs are needed to check the sensitivity of modelling results to these issues.

-**1.** Some previous studies have suggested that the MCM model may not work well for reproducing the HO$_x$ concentrations at high-BVOCs and low-NO$_x$ conditions, which seems to be the case of the study area in the present study. The authors may need to check the applicability of the MCM to the environmental condition at this forested mountain site.

Response: Many thanks and we agree with the referee that MCM needs to be improved and further optimized at pristine forest environments. And also as the OH mixing ratios modelled by PBM-MCM can only represent the levels at the site. Therefore, a parameterization method using measured aromatic hydrocarbons has been applied to estimate the regional mixing ratios of daytime OH radicals (Fig. 1 and Fig. 2) (Shiu et al., 2007). We think that this additional approach provides a good complement to the current model for evaluating the atmospheric oxidative capacity in the present forest regions. We have therefore added this point in the Section 2.4 and 3.3.1.

In the Section 2.4, Page 6:" Few previous studies have suggested that MCM may not work well for reproducing the OH concentrations in pristine forest environments (Kim et al., 2015). In addition, the OH mixing ratios modelled by the PBM-MCM can only represent the levels at the site. To provide a complement to the PBM-MCM, a widely-used parameterization method using measured aromatic hydrocarbons (i.e. BTEX, benzene, toluene, ethylbenzene, and m,p-xylene) was applied to estimate the regional mixing ratios of daytime OH (Shiu et al., 2007). The ratios of any two aromatics having the same emission sources but different photochemical reactivities can be used to measure photochemical oxidation (Parrish et al., 2007). This approach is based on three assumptions: (1) BTEX are removed from the atmosphere following pseudo-first-order kinetic; (2) no fresh BTEX are emitted to the air mass in the transport, and (3) the effects of horizontal and vertical mixing are similar for each compound. More details about the parameterization method are given in the Text S1."

In the Section 3.3.1, Page 9:"…To provide a complement to the PBM-MCM, regional mixing ratios of OH during 9:00-15:00 LST were calculated by a widely-used parameterization method using measured aromatic hydrocarbon ratios, i.e. toluene/benzene (T/B), ethylbenzene/benzene (E/B), and m,p-xylene/benzene (X/B) (Fig. S3). The average regional concentrations of OH during 9:00-15:00 LST

was $19.7 \pm 2.3 \times 10^6$ molecules cm^{-3}, even higher than the modelled site-level OH of $11.7 \pm 0.4 \times 10^6$ molecules cm^{-3}....".
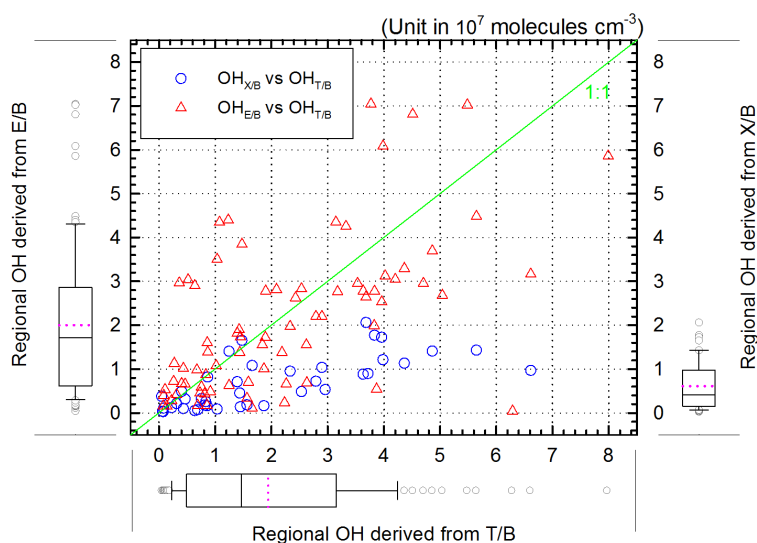

Fig. 1: Scatterplots of the regional mixing ratios of OH during 09:00–15:00 LST derived from the toluene/benzene (OH$_{T/B}$), ethylbenzene/benzene (OH$_{E/B}$) and m,p-xylene/benzene (OH$_{X/B}$) ratios. The green line denotes a 1:1 relationship. Next to axes are the box and whisker plots of each result, and the pink dotted lines denote the mean values.
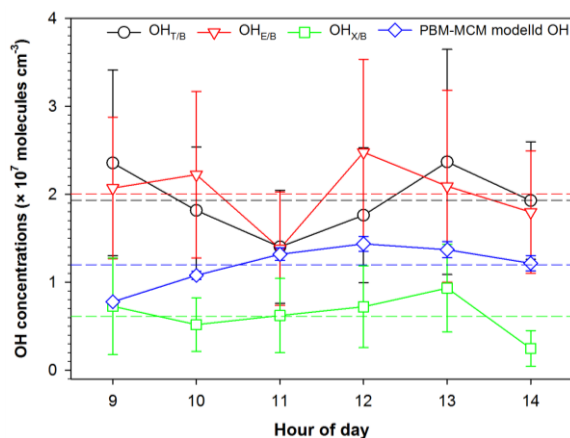

Fig. 2: Hourly variations of OH concentrations derived from the toluene/benzene ratio (OH$_{T/B}$), ethylbenzene/benzene ratio (OH$_{E/B}$), m,p-xylene/benzene ratio (OH$_{X/B}$) and PBM-MCM during 09:00 – 15:00 LST. Short-dashed lines denote the mean values of each method. Error bars indicate the 95% confidence interval.

References:

Shiu, C. J., Liu, S. C., Chang, C. C., Chen, J. P., Chou, C. C. K., Lin, C. Y., and Young, C. Y.: Photochemical production of ozone and control strategy for Southern Taiwan, Atmos Environ, 41, 9324-9340, 10.1016/j.atmosenv.2007.09.014, 2007.

Kim, S., Kim, S. Y., Lee, M., Shim, H., Wolfe, G. M., Guenther, A. B., He, A., Hong, Y., and Han, J.: Impact of isoprene and HONO chemistry on ozone and OVOC formation in a semirural South Korean forest, Atmos Chem Phys, 15, 4357-4371, 10.5194/acp-15-4357-2015, 2015.

-**2.** The NO_2 measurement analyzer used in this study may significantly overestimate for NO_2 at rural and remote sites. The authors are suggested to conduct more modeling analyses with artificially reduced NO_2 concentrations to examine the sensitivity of predicted OH and NO_3 to the input NO_2 data.

Response: Many thanks for spotting this, we have therefore conducted sensitivity analyses of modelled daytime OH and nighttime NO_3 with cutting NO_2 concentrations. The OH and NO_3 concentrations showed decreasing trends with the NO_2 reducing (Fig. 3). Assuming the average concentrations of daytime and nighttime NO_2 have been overestimated by 64.4 ± 2.9% and 62.4 ± 3.0% (Fig. 4), respectively, according to the results at a high-altitude mountain site in China (Xu et al., 2013), the mean daytime OH concentration at the present site would decrease from 7.3 ± 0.5 × 10^6 molecules cm^{-3} to 5.5 ± 0.4 × 10^6 molecules cm^{-3}, with a reduction rate of 23.8 ± 6.2%. And for nighttime NO_3, the decreasing rate was 41.5 ± 5.2% (from 6.0 ± 0.5 × 10^8 molecules cm^{-3} to 3.5 ± 0.3 × 10^8 molecules cm^{-3}). We have therefore added discussions about this point in the Section 2.3 and 3.3.3.

In the Section 2.3, Page 6: "…Sensitivity analyses were conducted for the model by varying the mixing ratios of NO_2…."

In the Section 3.3.3, Page 8: "Three issues should be noted in applying PBM-MCM to evaluate the AOC in the present study. First, the NO_2 concentrations, an important input into PBM-MCM, may be significantly overestimated at this remote mountaintop site that receives a considerable amount of photochemically aged air (Xu et al., 2013). Thus we conducted sensitivity analyses of modelled OH and NO_3 with artificially reduced NO_2 concentrations for the period Aug.11−Aug.15 2016. The OH and NO_3 concentrations decrease with cutting NO_2 (Fig. S4). According to a recent study conducted at Mount Tai (Xu et al., 2013), we assumed the daytime and nighttime NO_2 measurements were overestimated by 64.4 ± 2.9% and 62.4 ± 3.0%, respectively. Thus the recalculated mean daytime OH concentration would decrease from 7.3 ± 0.5 × 10^6 molecules cm^{-3} to 5.5 ± 0.4 × 10^6 molecules cm^{-3}, with a reduction

rate of 23.8 ± 6.2%. And for nighttime NO_3, the reduction rate was 41.5 ± 5.2% (from 6.0 ± 0.5 × 10^8 molecules cm^{-3} to 3.5 ± 0.3 × 10^8 molecules cm^{-3}).....".
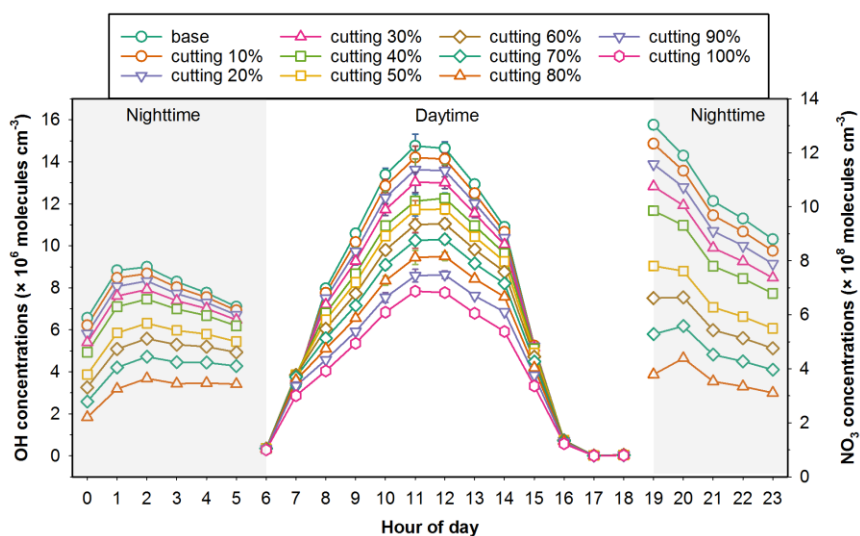

Fig. 3: Sensitivity analysis of PBM-MCM modelled daytime OH and nighttime NO_3 with reduced NO_2 concentrations for the period Aug 11 – Aug 15 2016.
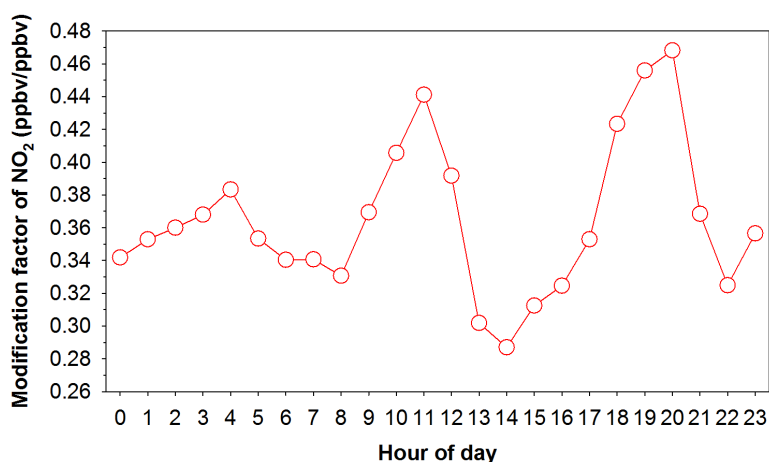

Fig. 4: Hourly modification factor of NO_2 during Jul 15–Aug 17 2016 at the Nanling site. The data in the figure are reproduced from the study conducted at a high-altitude mountain site (Mt. Tai) in central-eastern China by Xu et al. (2013).

References:

Xu, Z., Wang, T., Xue, L. K., Louie, P. K. K., Luk, C. W. Y., Gao, J., Wang, S. L., Chai, F. H., and Wang, W. X.: Evaluating the uncertainties of thermal catalytic conversion in measuring atmospheric nitrogen dioxide at four differently polluted sites in China, Atmos Environ, 76, 221-226, 10.1016/j.atmosenv.2012.09.043, 2013.

-**3.** The heterogeneous reactions of N_2O_5 play an important role in the nocturnal NO_3 chemistry. How does the PBM-MCM model present the N_2O_5 chemistry? What uptake coefficients of N_2O_5 onto particles were adopted in the model? Previous MCM modelling studies with addition of heterogeneous N_2O_5 chemistry have indicated the significant effect of this process on the simulation of photochemical processes (*Xue et al., 2014*). Additional modelling analyses are needed to examine the sensitivity of NO_3 to the N_2O_5 heterogeneous chemistry.

Response: We appreciate the referee's question and we agree that taking N_2O_5 heterogeneous chemistry into consideration would be very meaningfully. Unfortunately, we were not able to quantitatively take into account this important mechanism. We have admitted this limitation in the manuscript.

In the Section 2.3, Page 6: "It is noteworthy that … the heterogeneous process of N_2O_5 were not considered in the PBM-MCM.....".

In the Section 3.3.3, Page10-11: "…Finally, the dinitrogen pentoxides (N_2O_5) that formed from the oxidation of NO_2 by NO_3 can be taken up onto aerosols via heterogeneous reactions, which is an important sink of NO_2 and O_3 at night and can compete with the reactions of NO_3 with isoprene (Xue et al., 2014b;Brown et al., 2016;Millet et al., 2016). Unfortunately, we were not able to quantitatively take into account this important mechanism in this study, and further studies are needed to make up this limitation."

References:
Xue, L. K., Wang, T., Gao, J., Ding, A. J., Zhou, X. H., Blake, D. R., Wang, X. F., Saunders, S. M., Fan, S. J., Zuo, H. C., Zhang, Q. Z., and Wang, W. X.: Ground-level ozone in four Chinese cities: precursors, regional transport and heterogeneous processes, Atmos. Chem. Phys., 14, 13175-13188, 10.5194/acp-14-13175-2014, 2014b.
Millet, D. B., Baasandorj, M., Hu, L., Mitroo, D., Turner, J., and Williams, B. J.: Nighttime Chemistry and Morning Isoprene Can Drive Urban Ozone Downwind of a Major Deciduous Forest, Environ Sci Technol, 50, 4335-4342, 10.1021/acs.est.5b06367, 2016.
Brown, S. S., Dube, W. P., Tham, Y. J., Zha, Q. Z., Xue, L. K., Poon, S., Wang, Z., Blake, D. R., Tsui, W., Parrish, D. D., and Wang, T.: Nighttime chemistry at a high altitude site above Hong Kong, Journal of Geophysical Research-Atmospheres, 121, 2457-2475, 10.1002/2015jd024566, 2016.

-4. Similarly, the HONO chemistry was also not well represented in the MCM model, but plays an important role in the OH simulation (*Xue et al., 2014*). Did the PBM-MCM model take this chemistry into account? If not, the authors may need to conduct some sensitivity analyses or at least mention the potential uncertainty of modeling results.

Xue et al., Ground-level ozone in four Chinese cities: precursors, regional transport and heterogeneous processes, Atmos. Chem. Phys., 14, 13175- 13188, 2014.

Response: Many thanks for spotting this. Since we did not measure the concentrations of HONO in the sampling periods, the average diurnal profiles of HONO observed at a background site (Hok Tsui) in Hong Kong in autumn 2012 (Zha, 2015) were applied to conduct sensitivity analyses. The results showed that daytime OH concentrations with HONO taken into account was 22 ± 19% higher than that without HONO (Fig. 5). Nonetheless, the results are not representative due to the lack of HONO measurements at the present site. Thus, certain uncertainties remain and we have therefore added discussions about this point in the Section 2.3 and Section 3.3.3.

In the Section 2.3, Page 6: "…Sensitivity analyses were conducted for the model by varying the mixing ratios of … and HONO….".

In the Section 3.3.3, Page 10: "…Second, a number of studies have shown that HONO plays an important role in daytime OH formation (Xue et al., 2014b). As the concentrations of HONO were not measured in the sampling periods, we therefore conducted sensitivity analyses by using a two-day (Aug 13 and Aug 15) dataset coupled with the average diurnal profiles of HONO observed at a background site (Hok Tsui) in Hong Kong in autumn 2012 (Zha, 2015). The results showed that daytime OH concentrations with HONO considered was 22 ± 19% higher than that without HONO (Fig. S5)….".
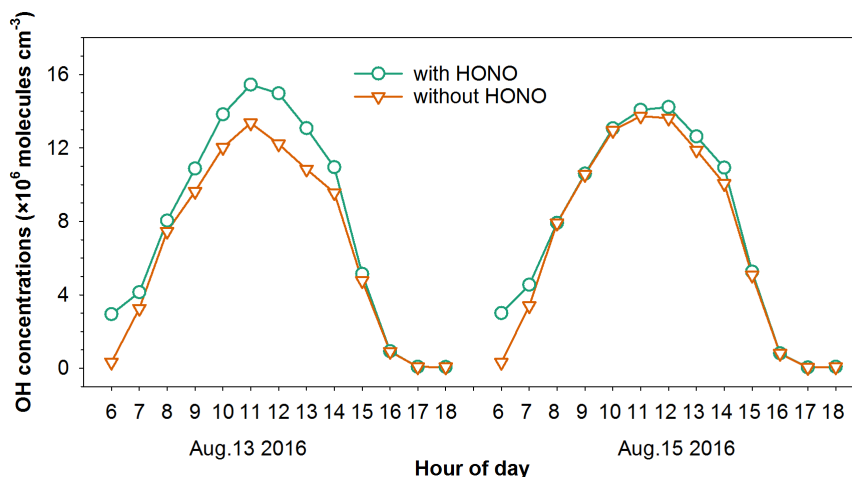
Fig. 5: Sensitivity analysis of PBM-MCM modelled daytime OH with and without HONO for the period Aug 13 and Aug 15 2016. The HONO data was obtained from the study conducted at a background site (Hok Tsui) in Hong Kong in autumn 2012 by Zha (2015).

References:

Zha, Q.: Measurement of nitrous acid (HONO) and the implications to photochemical pollution, MPhil dissertation, Department of Civil and Environmental Engineering, The Hong Kong Polytechnic University, 2015.

Xue, L. K., Wang, T., Gao, J., Ding, A. J., Zhou, X. H., Blake, D. R., Wang, X. F., Saunders, S. M., Fan, S. J., Zuo, H. C., Zhang, Q. Z., and Wang, W. X.: Ground-level ozone in four Chinese cities: precursors, regional transport and heterogeneous processes, Atmos. Chem. Phys., 14, 13175-13188, 10.5194/acp-14-13175-2014, 2014b.

-**5.** Sections 2.4 and 2.5: additional information about the calculation methods of the isoprene reaction time and air mass age, including principles and uncertainties, are required for readers to better understand and reproduce the results. The authors may also need to comment on the difference between reaction time and air mass age.

Response: Many thanks for spotting this. The description of the isoprene reaction time calculation have been modified and supplied in the Section 2.5 and Section 3.4. As we realized that the air mass age calculation was not closely related to the topic of the manuscript, this part has been removed out of the revised version.

In the Section 2.5, Page 7: "To check out the magnitude of isoprene oxidation, the initial isoprene was calculated using a "sequential reaction approach" based on the isoprene's oxidation mechanism and

an empirical relationship between isoprene and its first-stage oxidation products (*i.e.* MVK and MACR) (Wolfe et al., 2016). This simplified parameterization method is based on four assumptions: (1) no fresh emissions of isoprene are introduced and isoprene emissions are constant during the process; (2) there were no additional sources of MVK and MACR apart from the oxidation of isoprene; (3) the processing time of the air mass are identical for all three compounds; and (4) only purely chemical reactions are included and the effects of turbulent mixing, horizontal convection and deposition are not accounted for. More description of the calculation is given in the Text S2."

In the Section 3.4, Page 11: "Fig. 6 shows the derived isoprene reaction times (IRT) from [MVK]/[isoprene] and [MACR]/[isoprene], respectively. IRT derived from the two ratios exhibit a significant linear correlation (R^2=0.91 and 0.90 for daytime and nighttime, respectively). The IRT derived from [MACR]/[isoprene] is 13% lower than that from [MVK]/[isoprene] on average, and we use the mean of these two values. The median and mean IRT during the day is 0.27 and 1.39 hr, respectively, with 4.10 and 4.49 hr at night. The median daytime reaction time (0.27 hr) of measured isoprene was slightly lower than the theoretical lifetime of isoprene (0.40 hr at 12-h daytime averaged [OH] = 8.0×10^6 molecules cm^{-3}). The short reaction time of isoprene indicates fast isoprene oxidation at this mountaintop site."

References:

Wolfe, G. M., Kaiser, J., Hanisco, T. F., Keutsch, F. N., de Gouw, J. A., Gilman, J. B., Graus, M., Hatch, C. D., Holloway, J., Horowitz, L. W., Lee, B. H., Lerner, B. M., Lopez-Hilifiker, F., Mao, J., Marvin, M. R., Peischl, J., Pollack, I. B., Roberts, J. M., Ryerson, T. B., Thornton, J. A., Veres, P. R., and Warneke, C.: Formaldehyde production from isoprene oxidation across NOx regimes, Atmos Chem Phys, 16, 2597-2610, 10.5194/acp-16-2597-2016, 2016.

-**6.** The major conclusion of this study is the strong regional atmospheric oxidative capacity leads to fast oxidation of isoprene in southern China. Some recent long-term observational studies have indicated the increasing trends of ozone concentrations in this region (*Wang et al., 2009*; *Xue et al., 2014*). As ozone is usually regarded as an indicator of the regional atmospheric oxidation capacity, these studies confirmed the increasing trend of atmospheric oxidizing capacity in southern China. It would be useful if the authors could discuss the trends of ozone and atmospheric oxidative capacity and comment on the projected trend in the future.

Wang et al., Increasing surface ozone concentrations in the background atmosphere of southern China, 1994-2007. Atmos. Chem. Phys., 9, 6217-6227, 2009.

Xue et al., Increasing external effects negate local efforts to control ozone air pollution: a case study of Hong Kong and implications for other Chinese cities, Environ. Sci. Tech., 48, 10769-10775, 2014.

Response: Many thanks for spotting this. We have therefore added the following text to the revised manuscript in the Section 2.1 and Section 4, respectively.

In the Section 2.1, Page 4: "…Ground-level O_3, another indicator of the regional AOC, was also high in the PRD, with hourly mixing ratios of up to 220 ppbv (Wang et al., 2017b). Furthermore, O_3 in this region was observed to increase at a rate of 0.27 to 0.86 ppbv/year (Wang et al., 2009;Xue et al., 2014a;Wang et al., 2017c)…"

In the Section 4, Page 12: "Furthermore, recent long-term observational studies in the PRD (Wang et al., 2009;Xue et al., 2014a;Wang et al., 2017c;Wang et al., 2017b) have indicated the increasing trends of surface O_3, another indicator of the regional AOC.…"

References:

Wang, T., Wei, X. L., Ding, A. J., Poon, C. N., Lam, K. S., Li, Y. S., Chan, L. Y., and Anson, M.: Increasing surface ozone concentrations in the background atmosphere of Southern China, 1994-2007, Atmos Chem Phys, 9, 6217-6227, 2009.

Xue, L., Wang, T., Louie, P. K., Luk, C. W., Blake, D. R., and Xu, Z.: Increasing external effects negate local efforts to control ozone air pollution: a case study of Hong Kong and implications for other Chinese cities, Environ Sci Technol, 48, 10769-10775, 10.1021/es503278g, 2014a.

Wang, T., Xue, L., Brimblecombe, P., Lam, Y. F., Li, L., and Zhang, L.: Ozone pollution in China: A review of concentrations, meteorological influences, chemical precursors, and effects, The Science of the total environment, 575, 1582-1596, 10.1016/j.scitotenv.2016.10.081, 2017a.

Wang, Y., Wang, H., Guo, H., Lyu, X., Cheng, H., Ling, Z., Louie, P. K. K., Simpson, I. J., Meinardi, S., and Blake, D. R.: Long term O3-precursor relationships in Hong Kong: Field observation and model simulation, Atmospheric Chemistry and Physics Discussions, 1-29, 10.5194/acp-2017-235, 2017b.

-**7.** Page 1, Lines 22-23: this sentence is incomplete. Rephrase this sentence.

Response: Many thanks for spotting this, correction have been made to read "To investigate the atmospheric oxidative capacity (AOC) in forested high mountain areas adjacent to the photochemistry-active Pearl River Delta (PRD) region in southern China, one-month online

observations of isoprene and its oxidation products methyl vinyl ketone (MVK) and methacrolein (MACR) were conducted at a national background station in Nanling Mountains in summer 2016.".

-8. Page 2, Lines 27-31: the oxidation of isoprene by OH radicals is very complex. MACR and MVK can be further oxidized to form MGLY and other secondary compounds. Here it would be helpful to add several sentences to briefly summarize the thorough oxidation chemistry of isoprene as well as the major knowledge gaps in understanding this chemistry.

Response: Many thanks, we have therefore added brief descriptions and major gaps in this paragraph: "…In the real ambient environment, the major competing reaction pathways include both NO- and HO_2-channels which dominate in polluted and pristine atmospheres, respectively (Paulot et al., 2009;Su et al., 2016). The relative importance of the two pathways varies with NO_x (NO_x = NO + NO_2) mixing ratios. Ambient measurements in pristine Amazon forests demonstrated that high OH concentrations often occur under high-isoprene and low-NO_x (< 1 ppbv) conditions where OH regeneration contributes greatly to the oxidative capacity of the atmosphere (Lelieveld et al., 2008;Fuchs et al., 2013;Rohrer et al., 2014). Several recent studies have shown that small increases of NO_x concentration above the background level can lead to a large change in the oxidative capacity and chemistry of the forest atmosphere (Liu et al., 2016;Su et al., 2016;Santos et al., 2018;Liu et al., 2018). In addition, the high OH-recycling efficiency is not unique to pristine forests, an important but different OH-recycling mechanism has been discovered in an isoprene-emitting forest suffering from heavy air pollution (Hofzumahaus et al., 2009). Thus, it is vital to understand the isoprene photochemistry under moderately polluted forest atmospheric conditions with high isoprene emissions and a broad range of NO_x concentrations."

References:
Paulot, F., Crounse, J. D., Kjaergaard, H. G., Kurten, A., St Clair, J. M., Seinfeld, J. H., and Wennberg, P. O.: Unexpected epoxide formation in the gas-phase photooxidation of isoprene, Science, 325, 730-733, 10.1126/science.1172910, 2009.
Su, L. P., Patton, E. G., de Arellano, J. V. G., Guenther, A. B., Kaser, L., Yuan, B., Xiong, F. L. Z., Shepson, P. B., Zhang, L., Miller, D. O., Brune, W. H., Baumann, K., Edgerton, E., Weinheimer, A., Misztal, P. K., Park, J. H., Goldstein, A. H., Skog, K. M., Keutsch, F. N., and Mak, J. E.: Understanding isoprene

photooxidation using observations and modeling over a subtropical forest in the southeastern US, Atmos Chem Phys, 16, 7725-7741, 10.5194/acp-16-7725-2016, 2016.

Lelieveld, J., Butler, T. M., Crowley, J. N., Dillon, T. J., Fischer, H., Ganzeveld, L., Harder, H., Lawrence, M. G., Martinez, M., Taraborrelli, D., and Williams, J.: Atmospheric oxidation capacity sustained by a tropical forest, Nature, 452, 737-740, 10.1038/nature06870, 2008.

Fuchs, H., Hofzumahaus, A., Rohrer, F., Bohn, B., Brauers, T., Dorn, H. P., Haseler, R., Holland, F., Kaminski, M., Li, X., Lu, K., Nehr, S., Tillmann, R., Wegener, R., and Wahner, A.: Experimental evidence for efficient hydroxyl radical regeneration in isoprene oxidation, Nat Geosci, 6, 1023-1026, 10.1038/Ngeo1964, 2013.

Rohrer, F., Lu, K. D., Hofzumahaus, A., Bohn, B., Brauers, T., Chang, C. C., Fuchs, H., Haseler, R., Holland, F., Hu, M., Kita, K., Kondo, Y., Li, X., Lou, S. R., Oebel, A., Shao, M., Zeng, L. M., Zhu, T., Zhang, Y. H., and Wahner, A.: Maximum efficiency in the hydroxyl-radical-based self-cleansing of the troposphere, Nat Geosci, 7, 559-563, 10.1038/Ngeo2199, 2014.

Santos, F. C., Longo, K. M., Guenther, A. B., Kim, S., Gu, D., Oram, D. E., Forster, G. L., Lee, J., Hopkins, J. R., Brito, J. F., and Freitas, S. R.: Biomass burning emissions disturbances on the isoprene oxidation in a tropical forest, Atmospheric Chemistry and Physics Discussions, 2017, 1-35, 10.5194/acp-2017-1083, 2017.

Liu, Y., Brito, J., Dorris, M. R., Rivera-Rios, J. C., Seco, R., Bates, K. H., Artaxo, P., Duvoisin, S., Jr., Keutsch, F. N., Kim, S., Goldstein, A. H., Guenther, A. B., Manzi, A. O., Souza, R. A., Springston, S. R., Watson, T. B., McKinney, K. A., and Martin, S. T.: Isoprene photochemistry over the Amazon rainforest, Proc Natl Acad Sci U S A, 113, 6125-6130, 10.1073/pnas.1524136113, 2016.

Liu, Y., Seco, R., Kim, S., Guenther, A. B., Goldstein, A. H., Keutsch, F. N., Springston, S. R., Watson, T. B., Artaxo, P., Souza, R. A. F., McKinney, K. A., and Martin, S. T.: Isoprene photo-oxidation products quantify the effect of pollution on hydroxyl radicals over Amazonia, Science Advances, 4, 2018.

-9. Page 3, Lines 1-4: at nighttime, NO_3 is generally in a thermal equilibrium with N_2O_5, which can be also taken up onto aerosols. Such heterogeneous reaction of N_2O_5 is an important sink of NO_x at nighttime, and can compete with the reactions of NO_3 with BVOCs. The authors are suggested to add several sentences to mention this process and provide a thorough picture of the nocturnal chemistry.

Response: Many thanks and we have added this point in the Section 3.3.3, Page10-11: "…the dinitrogen pentoxides (N_2O_5) that formed from the oxidation of NO_2 by NO_3 can be taken up onto aerosols via heterogeneous reactions, which is an important sink of NO_2 and O_3 at night and can compete with the reactions of NO_3 with isoprene (Xue et al., 2014b;Brown et al., 2016;Millet et al., 2016)."

References:
Xue, L. K., Wang, T., Gao, J., Ding, A. J., Zhou, X. H., Blake, D. R., Wang, X. F., Saunders, S. M., Fan, S. J., Zuo, H. C., Zhang, Q. Z., and Wang, W. X.: Ground-level ozone in four Chinese cities: precursors,

regional transport and heterogeneous processes, Atmos. Chem. Phys., 14, 13175-13188, 10.5194/acp-14-13175-2014, 2014b.

Brown, S. S., Dube, W. P., Tham, Y. J., Zha, Q. Z., Xue, L. K., Poon, S., Wang, Z., Blake, D. R., Tsui, W., Parrish, D. D., and Wang, T.: Nighttime chemistry at a high altitude site above Hong Kong, Journal of Geophysical Research-Atmospheres, 121, 2457-2475, 10.1002/2015jd024566, 2016.

Millet, D. B., Baasandorj, M., Hu, L., Mitroo, D., Turner, J., and Williams, B. J.: Nighttime Chemistry and Morning Isoprene Can Drive Urban Ozone Downwind of a Major Deciduous Forest, Environ Sci Technol, 50, 4335-4342, 10.1021/acs.est.5b06367, 2016.

-**10.** Page 3, Lines 20-21: rephrase this sentence.

Response: Many thanks for spotting this, corrections have been made to read "This paper is structured as follows. Firstly, an overview of the meteorological and chemical conditions is given. Second, the measured concentrations and diurnal variations of isoprene and its oxidation products are presented. Then the estimated concentrations of daytime OH and nighttime NO_3 are presented and discussed in detail. And furthermore, the initial mixing ratios and atmospheric reaction time of isoprene were estimated. Finally, concluding remarks including a synthesis of current findings and some implications are presented. In this study, unexpected low isoprene levels and high (MVK+MACR)/isoprene ratios were observed. The subsequent theoretical calculations confirmed that the rapidly and highly isoprene oxidation might be attributable to a strong AOC in relation to the elevated regional complex air pollution in southern China."

-**11.** Page 4, Line 19: Southeast Asia

Response: Many thanks for spotting this – correction made.

-**12.** Change "atmospheric boundary layer (ABL)" to "planetary boundary layer (PBL)" throughout the manuscript.

Response: Many thanks, correction made.

-**13.** Page 5, Lines 18-19: it has been confirmed that this commercial NO_x analyzer with a default molybdenum oxide converter can significantly overestimate for NO_2, especially in rural and remote areas such as the forested mountaintop in the present study. The authors may need clarify the detailed configuration of this NO_x analyzer (e.g., the converters for converting NO_2 to NO) and state the uncertainty of NO_2 measurements if the MoO converter was used.

Xu et al., Evaluating the uncertainties of thermal catalytic conversion in measuring atmospheric nitrogen dioxide at four differently polluted sites in China, Atmos. Environ., 76, 221-226, 2013.

Response: We agree with the referee on the impact of molybdenum oxide converter may have on the measured NO_2 concentrations and we have added a discussion accordingly in the Section 2.2.2 and Section 3.1, respectively.

In the Section 2.2.2, Page 6: "NO_2 is converted to NO by a heated molybdenum converter before it can be measured by the chemiluminescence detection of NO. This method may cause an overestimation of NO_2 because the measured NO_2 probably includes some oxidized reactive nitrogen converted by the heated molybdenum (Xu et al., 2013). Thus, the NO_2 concentrations given below are considered as the upper limits of their actual values."

In the Section 3.1, Page 8: "Since the NO_2 concentrations measured by the molybdenum oxide converter technique can be significantly overestimated in areas far away from fresh NO_x emission sources (Xu et al., 2013), we corrected the observed NO_2 by adopting the hourly modification factors (Fig. S1) obtained at Mount Tai (1,533 m a.s.l.) in central-eastern China (Xu et al., 2013). The modified NO_2 (889 ± 27 pptv) was 1.1−2.5 times (1.8 ± 0.3) lower than that observed."

References:
Xu, Z., Wang, T., Xue, L. K., Louie, P. K. K., Luk, C. W. Y., Gao, J., Wang, S. L., Chai, F. H., and Wang, W. X.: Evaluating the uncertainties of thermal catalytic conversion in measuring atmospheric nitrogen dioxide at four differently polluted sites in China, Atmos Environ, 76, 221-226, 10.1016/j.atmosenv.2012.09.043, 2013.

-**14.** Page 7, Lines 7-9: it is a little bit strange that the observed concentrations of benzene (and also toluene) are very low. The lifetime of benzene is rather long and thus its ambient abundances are usually not so low.

Response: Thanks for your good question. We are also surprised by the low-level benzene and toluene, and the possible reasons may include:

(1) Long distance of the site away from city centers. The site is located in the free troposphere (FT) or upper planetary boundary layer (PBL) of southern China. Therefore, the low observed values suggest that the diffusion of benzene and toluene from ground source emissions within the PBL to the FT is strong, and thus they might have reached a steady state in this remote and high-elevation atmosphere.

(2) The strong oxidizing power of the troposphere in PRD region. Intensive studies have pointed to worsening photochemical pollution and strong atmospheric oxidative capacity throughout this region. Thus the chemical removal of benzene and toluene by radicals (e.g., OH) occurs rapidly and thoroughly along the paths air parcels traveled in the absence of mixing with fresh emissions in this pristine forest region.

(3) The high relative humidity (92.2 ± 8.3%) and cloudy conditions are favorable to the removal of benzene and toluene at this site, which may also lower the levels to a certain extent.

We have therefore added a discussion accordingly in the Section 3.1: "…Furthermore, anthropogenic tracers showed very low mixing ratios at this site. For example, the ambient aromatics levels at this site were significantly lower compared to the abundances that measured at a regional background site in the PRD (Wu et al., 2016). Toluene was the most abundant (154 ± 20 pptv), followed by benzene (51 ± 8 pptv), ethylbenzene (47 ± 6 pptv) and m,p-xylene (38 ± 4 pptv)."

References:
Wu, F., Yu, Y., Sun, J., Zhang, J., Wang, J., Tang, G., and Wang, Y.: Characteristics, source apportionment and reactivity of ambient volatile organic compounds at Dinghu Mountain in Guangdong Province, China, The Science of the total environment, 548-549, 347-359, 10.1016/j.scitotenv.2015.11.069, 2016.

-**15.** Page 7, Lines 9-11: provide standard deviations for the averages.

Response: Many thanks, done.

-**16.** Page 8, Lines 13-14: rephrase this sentence "Although …"

Response: Many thanks for spotting this, correction made.

-**17.** Page 8, Line 20: on the source of MVK and MACR at this site, I wonder if regional transport could also contribute to the observed MVK and MACR. What are the lifetimes of MVK and MACR?

Response: We appreciate the referee's question and the possible regional transport of MVK and MACR are explained in the following.

The lifetimes of MVK and MACR by reaction with OH are 1.9 and 1.0 hours, respectively, assuming 12-h daytime OH = 8.0×10^6 molecules cm^{-3}. The average daytime wind speed during the sampling periods was 3.9 $\pm$ 0.2 m s^{-1} at the site, and the distance between the sampling site and the nearest urban center is 38 km (Fig. 6), the air parcel from upwind locations would spend about 2.7 hours to arrive at the sampling site. This is enough time for the depletion of MVK and MACR along the traveling path during the daytime.

However, the nighttime chemical oxidation of MVK and MACR was slow, with lifetimes of MVK and MACR by NO_3 oxidation of 0.5 years and 72 hours, respectively, assuming 12-h nighttime NO_3 = 5.0×10^8 molecules cm^{-3}. Apart from biogenic sources, the anthropogenic sources of MVK and MACR, e.g., motor vehicles, biomass burning and industrial sources, have been reported by many studies (Borbon et al., 2001;Wagner and Kuttler, 2014;Hsieh et al., 2016;Diao et al., 2016). Therefore, the regional transport of MVK- or MACR- laden air could affect the observed nighttime levels at the site.

The "polarPlot" technique was therefore used for source identification (Fig. 7). The red dotted sectorial domains in the figure are interpreted as the regional transport interference as the concentrations of species increase with increasing wind speed. The high levels of species at high wind

speeds most likely came from the nearby urban centers. Therefore, measurements that are deemed to be affected by regional transport are all excluded from the dataset in the analysis.

We have therefore added a discussion accordingly in Section 3.2, Page 9: "…with little transported from anthropogenic sources in neighbor cities at night (see discussion in Text S3)."

Fig. 6: (a) Location of the Nanling site, Dinghu Mountain site, Hok Tsui site, Guangzhou and Hong Kong. The Nanling site is 174 km northeast to the Dinghu Mountain site 178 km northwest to Guangzhou. Red outlined domain represent the Pearl River Delta region. (b) Map showing the nearest urban centers (Yangshan County, Ruyuan County, Lechang City, Lianzhou City, Shaoguan City and Yingde City) around the site.
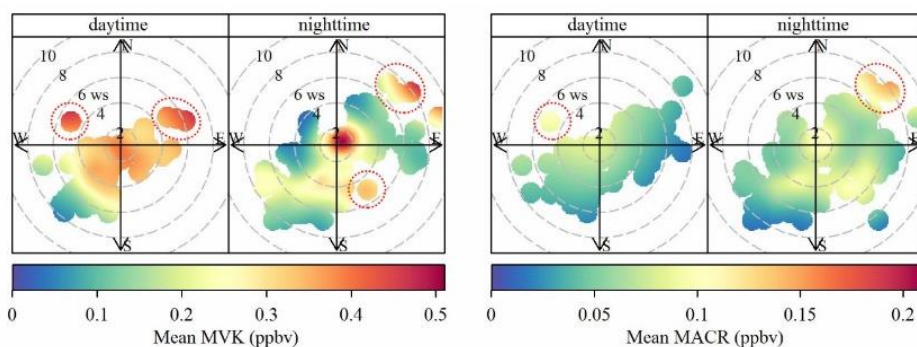
Fig. 7: Daytime and nighttime polarplots of MVK and MACR during the sampling period (July 15–August 17 2016). Concentrations varied by wind speed (ws, unit in m/s) and wind direction. Red dotted sectorial domains represent the interferences of regional transport from nearby urban centers.

References:

Borbon, A., Fontaine, H., Veillerot, M., Locoge, N., Galloo, J. C., and Guillermo, R.: An investigation into the traffic-related fraction of isoprene at an urban location, Atmos Environ, 35, 3749-3760, Doi 10.1016/S1352-2310(01)00170-4, 2001.

Wagner, P., and Kuttler, W.: Biogenic and anthropogenic isoprene in the near-surface urban atmosphere: A case study in Essen, Germany, Science of The Total Environment, 475, 104-115, http://dx.doi.org/10.1016/j.scitotenv.2013.12.026, 2014.

Hsieh, H., Ouyang, C., and Wang, J.: Revelation of Coupling Biogenic with Anthropogenic Isoprene by Highly Time-Resolved Observations, Aerosol and Air Quality Research, 10.4209/aaqr.2016.04.0133, 2016.

Diao, L. J., Choi, Y., Czader, B., Li, X. S., Pan, S., Roy, A., Souri, A. H., Estes, M., and Jeon, W.: Discrepancies between modelled and observed nocturnal isoprene in an urban environment and the possible causes: A case study in Houston, Atmos Res, 181, 257-264, 10.1016/j.atmosres.2016.07.009, 2016.

-**18.** Page 10, Line 17, "the observed relationship of observed MVK/isoprene": delete one "observed"

Response: Many thanks, correction made.

-**19.** Table 1: provide the standard deviation of the average concentrations if available.

Response: Many thanks, done.

Comments by Referee #3:

Gong et al. presents their results of online observations of isoprene and its first-stage oxidation products MVK and MACR in summer 2016 at a remote, high-altitude mountain forest site to the north of the air-polluted PRD region in southern China. They found that the isoprene level was significantly lower and attributed it to the strong regional atmospheric oxidative capacity. The PBM-MCM model was used to estimate the OH and NO_3 concentrations to support their assumptions. The paper is well written and organized. The reviewer would recommend the manuscript for publication after some specific comments.

Response: We thank the referee for this overview. We have made changes to the manuscript based on the referee's helpful comments.

-**1.** O_3, OH_x, PAN, and NO_3 are indicators of atmospheric oxidative capacity. Since OH and NO_3 were not determined in the observation, the observed O_3 concentration is a more powerful tool to express the atmospheric oxidative capacity. The diurnal variations of O_3 peaked at 20:00 is very interesting, because the changing trends of O_3 and sun radiation were not accordant. The temporal variations of O_3 also show different trends during the observation. Could regional transport contribute O_3 to the measurement site? The authors had better add more discussion on the variations of O_3 concentration.

Response: Many thanks for spotting this. We noticed that the high levels of O_3, as well as its distinct diurnal variations, were observed at the site, and we are preparing another paper to discuss these points in details. In this revised manuscript, discussions about the high abundances of O_3 at the site has been added in the Section 3.1. As for the interesting O_3 diurnal variations, a number of studies have observed a similar pattern at mountaintops, that is, high concentrations at night and low concentrations during the daytime (Gallardo et al., 2000;Gao et al., 2017). Some previous studies have concluded that the factors closely related to the distinct O_3 diurnal patterns at mountaintops were the boundary layer diurnal cycles (Gao et al., 2017), the mountain-valley breezes (Zaveri et al., 1995;Yang et al., 2012;Cristofanelli et al., 2013), the regional transport effects (Naja et al., 2003;Li et al., 2008;Zhang et al., 2015;Gao et al., 2017), the location and altitude of a mountain (Chevalier et al.,

2007;Monteiro et al., 2012), and ozone vertical distributions (Forrer et al., 2000;Zellweger et al., 2003;Gheusi et al., 2011). Overall, the distinct diurnal variations in O_3 concentrations are the result of a combination of various physical and chemical processes. This point has been added to the Section 3.2.

In the Section 3.1, Page 7-8:" Similar as previous mountaintop studies, a distinct O_3 diurnal variation featured with high levels at night and low levels during the daytime (Zaveri et al., 1995;Gao et al., 2017) was observed in this study, most likely due to a combination of various physical and chemical processes (*e.g.* boundary layer diurnal cycles, mountain-valley breezes, regional transport, photochemical reactions)."

In the Section 3.2, Page 8:" High abundances of O_3 at this site likely indicate strong oxidizing power of the present forest atmospheres."

References:

Zaveri, R. A., Saylor, R. D., Peters, L. K., McNider, R., and SonG, A.: A model investigation of summertime diurnal ozone behavior in rural mountainous locations, Atmos Environ, 29, 1043-1065, 1995.

Forrer, J., Ruttimann, R., Schneiter, D., Fischer, A., Buchmann, B., and Hofer, P.: Variability of trace gases at the high-Alpine site Jungfraujoch caused by meteorological transport processes, Journal of Geophysical Research-Atmospheres, 105, 12241-12251, Doi 10.1029/1999jd901178, 2000.

Gallardo, L., Carrasco, J., and Olivares, G.: An analysis of ozone measurements at Cerro Tololo (30 degrees S, 70 degrees W, 2200 m.a.s.l.) in Chile, Tellus Series B-Chemical and Physical Meteorology, 52, 50-59, DOI 10.1034/j.1600-0889.2000.00959.x, 2000.

Naja, M., Lal, S., and Chand, D.: Diurnal and seasonal variabilities in surface ozone at a high altitude site Mt Abu (24.6 degrees N, 72.7 degrees E, 1680 m asl) in India, Atmos Environ, 37, 4205-4215, 10.1016/s1352-2310(03)00565-x, 2003.

Zellweger, C., Forrer, J., Hofer, P., Nyeki, S., Schwarzenbach, B., Weingartner, E., Ammann, M., and Baltensperger, U.: Partitioning of reactive nitrogen (NO_y) and dependence on meteorological conditions in the lower free troposphere, Atmos Chem Phys, 3, 779-796, 2003.

Chevalier, A., Gheusi, F., Delmas, R., Ordonez, C., Sarrat, C., Zbinden, R., Thouret, V., Athier, G., and Cousin, J. M.: Influence of altitude on ozone levels and variability in the lower troposphere: a ground-based study for western Europe over the period 2001-2004, Atmos Chem Phys, 7, 4311-4326, DOI 10.5194/acp-7-4311-2007, 2007.

Li, J., Pochanart, P., Wang, Z. F., Liu, Y., Yamaji, K., Takigawa, M., Kanaya, Y., and Akimoto, H.: Impact of Chemical Production and Transport on Summertime Diurnal Ozone Behavior at a Mountainous Site in North China Plain, Sola, 4, 121-124, 10.2151/sola.2008-031, 2008.

Gheusi, F., Ravetta, F., Delbarre, H., Tsamalis, C., Chevalier-Rosso, A., Leroy, C., Augustin, P., Delmas, R., Ancellet, G., Athier, G., Bouchou, P., Campistron, B., Cousin, J. M., Fourmentin, M., and Meyerfeld, Y.:

Pic 2005, a field campaign to investigate low-tropospheric ozone variability in the Pyrenees, Atmos Res, 101, 640-665, 10.1016/j.atmosres.2011.04.014, 2011.

Monteiro, A., Strunk, A., Carvalho, A., Tchepel, O., Miranda, A. I., Borrego, C., Saavedra, S., Rodriguez, A., Souto, J., Casares, J., Friese, E., and Elbern, H.: Investigating a high ozone episode in a rural mountain site, Environmental pollution, 162, 176-189, 10.1016/j.envpol.2011.11.008, 2012.

Yang, C. F. O., Lin, N. H., Sheu, G. R., Lee, C. T., and Wang, J. L.: Seasonal and diurnal variations of ozone at a high-altitude mountain baseline station in East Asia, Atmos Environ, 46, 279-288, 10.1016/j.atmosenv.2011.09.060, 2012.

Cristofanelli, P., di Carlo, P., Altorio, A., Dari Salisburgo, C., Tuccella, P., Biancofiore, F., Stocchi, P., Verza, G. P., Landi, T. C., Marinoni, A., Calzolari, F., Duchi, R., and Bonasoni, P.: Analysis of Summer Ozone Observations at a High Mountain Site in Central Italy (Campo Imperatore, 2388 m a.s.l.), Pure Appl. Geophys., 170, 1985-1999, 10.1007/s00024-012-0630-1, 2013.

Zhang, L., Jin, L. J., Zhao, T. L., Yin, Y., Zhu, B., Shan, Y. P., Guo, X. M., Tan, C. H., Gao, J. H., and Wang, H. L.: Diurnal variation of surface ozone in mountainous areas: Case study of Mt. Huang, East China, Science of the Total Environment, 538, 583-590, 10.1016/j.scitotenv.2015.08.096, 2015.

Gao, J., Zhu, B., Xiao, H., Kang, H., Hou, X., Yin, Y., Zhang, L., and Miao, Q.: Diurnal variations and source apportionment of ozone at the summit of Mount Huang, a rural site in Eastern China, Environmental pollution, 222, 513-522, 10.1016/j.envpol.2016.11.031, 2017.

-**2.** The modelled OH and NO_3 concentrations were regarded as the most important evidence for the conclusion of this manuscript. However, the PBM-MCM model is not a good tool to estimate OH concentrations at low NO_x concentrations at remote site like this study. The reviewer strongly recommend the authors add some other models to support their conclusions.

Response: Thanks for this comment. We agree with the referee that PBM-MCM indeed needs improvement and further optimization for its application under low-NO_x environments.

Thus on one hand we conducted sensitivity analyses of the PBM-MCM modelled OH concentrations with certain uncertainties. The results showed that the current PBM-MCM may have 19 ± 9% overestimation of the daytime OH mixing ratios at the present study. See also our response to Referee #2, comment #2 and #4 for more detailed discussion on this point.

On the other hand, a widely-used parameterization method with measured aromatic hydrocarbons has been applied to estimate the regional mixing ratios of daytime OH radicals (Shiu et al., 2007). This additional approach can provide a good complement to the current model for evaluating the atmospheric oxidative capacity in the present forest regions. We have therefore added this point in

21

the revised manuscript and supplement. See also our response to Referee #2, comment #1 for more detailed discussion of this point.

We sincerely appreciate the suggestions made by the Referees, and agree that more observations and modeling studies will be needed to address this question. We will consider the application of other models as a better diagnostic tool in the future, e.g., OBM-AOCP (Observation-Based Model for investigating Atmospheric Oxidative Capacity and Photochemistry) developed by Xue et al. (2016).

References:
Shiu, C. J., Liu, S. C., Chang, C. C., Chen, J. P., Chou, C. C. K., Lin, C. Y., and Young, C. Y.: Photochemical production of ozone and control strategy for Southern Taiwan, Atmos Environ, 41, 9324-9340, 10.1016/j.atmosenv.2007.09.014, 2007.
Xue, L. K., Gu, R. R., Wang, T., Wang, X. F., Saunders, S., Blake, D., Louie, P. K. K., Luk, C. W. Y., Simpson, I., Xu, Z., Wang, Z., Gao, Y., Lee, S. C., Mellouki, A., and Wang, W. X.: Oxidative capacity and radical chemistry in the polluted atmosphere of Hong Kong and Pearl River Delta region: analysis of a severe photochemical smog episode, Atmos Chem Phys, 16, 9891-9903, 10.5194/acp-16-9891-2016, 2016.

-**3.** Page 1, Line 22-23, this sentence is incomplete.

Response: Many thanks for spotting this, the correction has been made to read "To investigate the atmospheric oxidative capacity (AOC) in forested high mountain areas adjacent to the photochemistry-active Pearl River Delta (PRD) region in southern China, one-month online observations of isoprene and its oxidation products methyl vinyl ketone (MVK) and methacrolein (MACR) were conducted at a national background station in Nanling Mountains in summer 2016.".

-**4.** Page 4, Line 32, the specifications of the Teflon filter should be clarified.

Response: Many thanks for spotting this, corrections have been made to read "…a Teflon filter (0.25 µm pore size, 47 mm OD, Millipore, USA) was placed in front of the sample inlet."

-**5.** Page 5, Line 21-23, it is confused that "daily" and "every two days". Secondly, it seems that SO_2, NO_x, and CO analyzers are usually calibrated with domestic standard gases which are not NIST-traceable. The NIST-traceable standard was only applied to calibrate O_3 analyzer.

Response: Many thanks for spotting this mistake, corrections have been made to read "All instruments were calibrated weekly by using a multi-gas calibrator (Model 146i, Thermo Scientific, Inc.) throughout the study. The NIST-traceable (National Institute of Standards and Technology, USA) standard was applied to calibrate the O_3 analyzer. For the calibration of NO_x, SO_2 and CO analyzers, standard gases provided by NRCCRM (National Research Center for Certified Reference Materials, China) were applied. Zero and span checks of all analyzers were performed every two days.".

Low-level <u>summertime</u> isoprene observed ~~during summertime~~ at a forested mountaintop site in southern China: <u>Implications</u> for strong regional atmospheric oxidative capacity

Daocheng Gong[1,#], Hao Wang[1,2,#], Shenyang Zhang[1], Yu Wang[3], Shaw <u>Chen</u> Liu[1], Hai Guo[3], Min Shao[1], Congrong He[2,4], Duohong Chen[5], Lingyan He[6], Lei Zhou[1], Lidia Morawska[2,4], Yuanhang Zhang[7], Boguang Wang[1,2,*]

[1]Institute for Environmental and Climate Research, Jinan University, Guangzhou 511443, China
[2]JNU−QUT Joint Laboratory for Air Quality Science and Management, Jinan University, Guangzhou 511443, China
[3]Air Quality Studies, Department of Civil and Environmental Engineering, The Hong Kong Polytechnic University, Hung Hom, Hong Kong
[4]International Laboratory for Air Quality and Health, Queensland University of Technology, GPO Box 2434, Brisbane, Queensland 4001, Australia
[5]State Environmental Protection Key Laboratory of Regional Air Quality Monitoring, Guangdong Environmental Monitoring Center, Guangzhou 510308, China
[6]Key Laboratory for Urban Habitat Environmental Science and Technology, School of Environment and Energy, Peking University Shenzhen Graduate School, Shenzhen 518055, China
[7]State Key Joint Laboratory of Environmental Simulation and Pollution Control, College of Environmental Sciences and Engineering, Peking University, Beijing 100871, China

[#] These authors contributed equally to this work

Correspondence to: Boguang Wang (tbongue@jnu.edu.cn)

Abstract

<u>To investigate the atmospheric oxidative capacity (AOC) in forested high mountain areas adjacent to the photochemistry-active Pearl River Delta (PRD) region in southern China, one-month online observations of isoprene and its oxidation products methyl vinyl ketone (MVK) and methacrolein (MACR) were conducted at a national background station in Nanling Mountains in summer 2016.</u> The results showed that the observed daytime isoprene levels <u>(377 ± 46 pptv)</u> were significantly lower in comparison with other forest sites within and outside China, although the sampling site was surrounded with subtropical evergreen broad-leaved trees which are strong isoprene emitters. Also, high daytime (MVK+MACR)/isoprene ratios <u>(1.9 ± 0.5)</u> were observed. Based on the observations, we hypothesized that the lower isoprene levels in the study forest might be attributable to a strong AOC in relation to the elevated regional complex air pollution. In further data analyses, high site-level concentrations of daytime OH <u>(7.3 ± 0.5 × 10⁶ molecules cm⁻³)</u> and nighttime NO$_3$ radical <u>(6.0 ± 0.5 × 10⁸ molecules cm⁻³)</u> were estimated by using a photochemical box model incorporating Master Chemical Mechanism (PBM-MCM), <u>and high regional mixing ratios of OH (19.7 ± 2.3 × 10⁶ molecules cm⁻³) during 09:00-15:00 LST were also obtained by applying a parameterization method with measured aromatic hydrocarbons.</u> And besides, high initial mixing

ratios (1213 ± 108 pptv) and short atmospheric reaction time (0.27 hr) of isoprene during the day were derived by a sequential reaction approach. All these indicate that isoprene was rapidly and highly oxidized in this forest, which supports our hypothesis. The study suggests that the complex air pollution in the PRD may has significantly elevated the background AOC of the adjacent forests, and probably affects the regional air quality and ecological environment in the long term. The feedback of forest ecosystems to the increasing AOC in southern China warrants further studies.

Keywords: biogenic VOCs; isoprene; atmospheric oxidative capacity; Nanling Mountains; Pearl River Delta

1 Introduction

Isoprene (2-methyl-1,3-butadiene) is the most abundant non-methane volatile organic compound (NMVOC) in the atmosphere (Guenther et al., 2012). The high abundance and reactive chemistry of isoprene affect the oxidative capacity of the troposphere and contribute to the formation of ozone (O_3) and secondary organic aerosols (Claeys et al., 2004;Hewitt et al., 2011). The biogenic sources from terrestrial vegetation contribute more than 90% of atmospheric isoprene, with the largest contribution from forests (Guenther et al., 2006).

Isoprene emissions from forests have been extensively studied over the past decades (Thomas D Sharkey and Yeh, 2003). More recent works have expanded the focus from emissions (Gu et al., 2017) to impacts of isoprene on regional forest chemistry (Taraborrelli et al., 2012;Liu et al., 2016;Liu et al., 2018). These studies have greatly improved our understanding on oxidation process of isoprene, revealed current uncertainties associated with isoprene emission rates and degradation schemes, and highlighted the biogenic−anthropogenic interactions in moderately polluted forests (Rohrer et al., 2014). Recent studies in pristine Amazon forests have reported the disturbance of anthropogenic influence to the oxidation of isoprene and the amplification of atmospheric oxidative capacity (AOC) (Liu et al., 2016;Liu et al., 2018). However, studies on this kind of disturbance and amplification in certain polluted isoprene-rich environments such as the forests surrounding megacities remain scarce (Hofzumahaus et al., 2009).

Isoprene can be rapidly removed by oxidation of hydroxyl radicals (OH), once being released into the troposphere during the day. The oxidation is usually initiated by additional reaction of an OH across the double bond and followed by fast reaction with molecular oxygen. A population of hydroxyl-substituted isoprene peroxyl radicals (ISOPOO) is thereby produced (Orlando and Tyndall, 2012). The subsequent chemistry of the ISOPOO proceeds along several competing pathways (Jenkin et al., 2015). In the real ambient environment, the major competing reaction pathways include both NO- and HO_2-channels which dominate in polluted and pristine atmospheres, respectively (Paulot et al., 2009;Su et al., 2016). The relative importance of the two pathways varies with NO_x (NO_x = NO + NO_2) mixing ratios. Ambient measurements in pristine Amazon forests demonstrated that high OH concentrations often occur under high-isoprene and low-NO_x (< 1 ppbv) conditions where OH regeneration contributes greatly to the oxidative capacity of the atmosphere (Lelieveld et al.,

2008;Fuchs et al., 2013;Rohrer et al., 2014). Several recent studies have shown that small increases of NO_x concentration above the background level can lead to a large change in the oxidative capacity and chemistry of the forest atmosphere (Liu et al., 2016;Su et al., 2016;Santos et al., 2018;Liu et al., 2018). In addition, the high OH-recycling efficiency is not unique to pristine forests, an important but different OH-recycling mechanism has been discovered in an isoprene-emitting forest suffering from heavy air pollution (Hofzumahaus et al., 2009). Thus, it is vital to understand the isoprene photochemistry under moderately polluted forest atmospheric conditions with high isoprene emissions and a broad range of NO_x concentrations.

In moderately polluted environments, *e.g.* forests surrounding urban areas, nitrate radicals (NO_3) which form mainly from the oxidation of NO_2 by O_3 are the dominant oxidant of isoprene at night when photochemical production of OH have diminished (Ng et al., 2017). The nitrate radical can be abundant at night and short lived during the day due to its rapid photolysis in sunlight and its reaction with NO (Wayne et al., 1991). While nighttime isoprene emissions are negligible, isoprene emitted in the late afternoon can accumulate in the nighttime atmosphere. Organic nitrates produced from the isoprene+NO_3 reaction will be abundant enough to affect the nighttime radical chemistry and to persist into daytime where they may serve as NO_x reservoir (Perring et al., 2009). Therefore, isoprene NO_3 chemistry is important for understanding the nighttime oxidative capacity in moderately polluted forest atmospheres.

Methyl vinyl ketone (MVK) and methacrolein (MACR) are key intermediates generated from isoprene oxidation with OH and NO_3 (Sprengnether et al., 2002;Perring et al., 2009). The sum of MVK and MACR accounts for about 80% of the carbon in the initial stage of isoprene oxidation in the atmosphere (Jenkin et al., 2015). Field measurements of MVK and MACR have been widely conducted during the past decades to explore the oxidation mechanisms of isoprene in forested environments (Stroud et al., 2001;Apel et al., 2002;Kuhn et al., 2007;Kalogridis et al., 2014;Liu et al., 2016;Santos et al., 2018;Liu et al., 2018). Few studies, however, have been performed at high-altitude mountain sites to investigate the influence of anthropogenic emissions to the isoprene oxidation and to evaluate the regional AOC (Reissell and Arey, 2001;Dreyfus et al., 2002;Guo et al., 2012). In this study, to deepen the scientific understanding of the isoprene oxidation and the background AOC on a regional scale, measurements of isoprene and its oxidation products were performed in Nanling mountains during the summer of 2016. To our knowledge, this was the first study of isoprene observation at remote and forested mountaintop site in southern China.

This paper is structured as follows. Firstly, an overview of the meteorological and chemical conditions is given. Second, the measured concentrations and diurnal variations of isoprene and its oxidation products are presented. Then the estimated concentrations of daytime OH and nighttime NO_3 are presented and discussed in detail. And furthermore, the initial mixing ratios and atmospheric reaction time of isoprene were estimated. Finally, concluding remarks including a synthesis of current findings and some implications are presented. In this study, unexpected low isoprene levels and high (MVK+MACR)/isoprene ratios were observed. The subsequent theoretical calculations confirmed that the rapidly and highly

isoprene oxidation might be attributable to a strong AOC in relation to the elevated regional complex air pollution in southern China.

2 Methods

2.1 Site description

The observations were conducted at a national background station in the Nanling Mountains that adjacent to the photochemistry-active Pearl River Delta (PRD) region in southern China. The PRD has become one of the most air-polluted areas in China, which happened along with rapid economic growth and urbanization over the past few decades (Chan and Yao, 2008). A number of studies have pointed to worsening photochemical pollution in this region (Wang et al., 2009;Zheng et al., 2010;Li et al., 2018). Highest ever-reported concentrations of OH have been observed in the PRD by recent studies (Hofzumahaus et al., 2009;Lu et al., 2012;Lu et al., 2014), indicating the strong AOC in this region. Limited studies of NO_3 oxidation chemistry have also confirmed considerable potential of NO_3 for the strong nighttime and even daytime atmospheric oxidative capacities in the PRD (Xue et al., 2016;Brown et al., 2016;Li et al., 2018). Ground-level O_3, another indicator of the regional AOC, was also high in the PRD, with hourly mixing ratios of up to 220 ppbv (Wang et al., 2017b). Furthermore, O_3 in this region was observed to increase at a rate of 0.27 to 0.86 ppbv/year (Wang et al., 2009;Xue et al., 2014a;Wang et al., 2017c). All these studies consistently demonstrate strong and enhancing AOC in the PRD.

To the north of the PRD lies the Nanling Mountains, an important geographic boundary in southern China separating the temperate areas in the north from subtropical regions in the southeast coast. The mountain range straddles more than 1,000 km from west to east across the borders of four provinces (*i.e.* Guangxi, Hunan, Guangdong and Jiangxi). Influenced by the East Asian monsoons, the area is the key pathway for the long-range transport of air pollutants between southern and middle-eastern China, making it a suitable location to monitor the regional background air quality. With a forest area of 5.36 million hectares, the Nanling Mountains holds the best preserved and the most representative subtropical forest in the regions of the same latitude in the world. The trees and shrubs in this region are mainly composed of subtropical evergreen broad-leaved and Moso bamboo forests (SFAPRC, 2014), both of which are well known to be strong isoprene emitters (Bai et al., 2016;Bai et al., 2017). Therefore, the Nanling Mountains is an ideal location for exploring anthropogenic−biogenic interactions because of its high natural emissions and its proximity to anthropogenic pollution sources. So far, however, no isoprene measurements have been conducted in this important area.

The sampling site (24° 41′ 56″ N, 112° 53′ 56″ E, 1,690 m a.s.l.) located at the summit of Mt. Tian Jing in the southern slope of the Nanling Mountains (Fig. 1) is ~15 m above the forest canopy. The site is far from urban and industrial areas, and free of any emissions from local anthropogenic activities. Mt. Tian Jing is the highest mountain within a radius of 24 km, with no obstacles around. To the south are the city clusters of the PRD (178 km north of the metropolitan Guangzhou). During the East Asian summer monsoon seasons (Jun to Sep), polluted air from the PRD or even Southeast Asia may reach the sampling site. As the Nanling site is a high-altitude mountaintop site in a remote region, and highly representative of the

1 upper planetary boundary layer (PBL) or lower free troposphere (FT) in southern China, measurements of surface isoprene

2 and other species can well represent a large-scale situation.

3 **2.2 Measurement Techniques**

4 **2.2.1 Sampling and analysis of VOCs**

5 The continuous sampling and analysis of ambient VOCs at the Nanling site were conducted automatically by a state-of-the-

6 art online cryogen-free GC−MS system with a time resolution of 1 hr in summer 2016 (*i.e.* Jul 15–Aug 17). The VOC

7 measurement instruments were deployed inside a two-story building. The inlet of sampling tube was located 1.5 m above the

8 rooftop of the building. Ambient air samples were drawn through a 5 m perfluoroalkoxy tube (OD 1/4 inch). The system

9 consisted of a cryogen-free trap pre-concentration device (TH-PKU 300B, Wuhan Tianhong Instrument Co. Ltd., China) and

10 a gas chromatography-mass spectrometry (7820A GC, 5977E MSD, Agilent Technologies Inc., USA). The details of this

11 system are described elsewhere (Wang et al., 2014). Briefly, the ambient air was sampled and pumped into an electronic

12 refrigeration and pre-concentration system at a flow rate of 60 mL/min for the second five minutes of each hour. In order to

13 prevent particulate matters from entering into the sampling system, a Teflon filter (0.25 μm pore size, 47 mm OD, Millipore,

14 USA) was placed in front of the sample inlet. Moisture and CO_2 were removed before VOC analysis by a water management

15 trap and a soda asbestos tube, respectively. VOCs were separated on a semipolar column (DB-624, 60 m × 0.25 mm ID × 1.4

16 μm, Agilent Technologies Inc., USA) and then quantified using a quadrupole MS detector with a full-scan mode. The GC

17 oven temperature was programmed initially at 38 °C for 3.5 min, increasing to 180 °C at a rate of 6 °C min^{-1} and holding for

18 15 min. The entire process took about 43 min.

19 Rigorous QA (quality assurance) and QC (quality control) procedures were performed through the entire measurement

20 period. To assess the wall loss of VOCs when air passing through the sampling tube, canister sampling at the sampling tube

21 inlet was conducted simultaneously with the online measurements, and samples were analysed using the offline mode of the

22 instrument at night of the same day. Twenty-four off-line samples were collected by canisters during the campaign. The

23 slope and correlation coefficient (R^2) of a plot between off-line samples and online measurements for isoprene, MVK and

24 MACR is 0.98–1.01 and >0.99, respectively. Calibration curves were established for each individual species at seven

25 different concentrations ranging from 10 to 2,000 pptv before sample analysis. The GC−MS system was also calibrated

26 using four internal standards (Bromochloromethane, 1,4-Difluorobenzene, Chlorobenzene-d5 and 4-Bromofluorobenzene).

27 A mixture of 57 non-methane hydrocarbons and a mixture of oxygenated VOCs (Linde Electronics and Specialty Gases,

28 USA) were used to make the standard curves for calibration. R^2 values of calibration curves were >0.99 for all species. Daily

29 calibrations were performed with ±10% variations with reference to the calibration curve results. The method detection limit

30 (MDL) for isoprene, MVK and MACR quantified with this system was 4, 15 and 10 pptv, respectively.

2.2.2 Measurements of trace gases and meteorological parameters

Ozone (O_3) was measured using a commercial UV photometric instrument (Model 49i, Thermo Scientific, Inc.), which has a detection limit of 0.5 ppbv. Oxides of nitrogen ($NO-NO_2-NO_x$) were measured at 1 min resolution using chemiluminescence analyser (Model 42i-TL, Thermo Scientific, Inc.), which has a detection limit of 0.05 ppbv. NO_2 is converted to NO by a heated molybdenum converter before it can be measured by the chemiluminescence detection of NO. This method may cause an overestimation of NO_2 because the measured NO_2 probably includes some oxidized reactive nitrogen converted by the heated molybdenum (Xu et al., 2013). Thus, the NO_2 concentrations given below are considered as the upper limits of their actual values. Sulfur dioxide (SO_2) was measured by pulsed UV fluorescence (Model 43i-TLE, Thermo Scientific, Inc.) with a detection limit of 0.05 ppbv. Carbon monoxide (CO) was monitored using a gas filter correlation infrared absorption trace level analyser (Model 48i-TLE, Thermo Scientific, Inc.). All instruments were calibrated weekly by using a multi-gas calibrator (Model 146i, Thermo Scientific, Inc.) throughout the study. The NIST-traceable (National Institute of Standards and Technology, USA) standard was applied to calibrate the O_3 analyser. For the calibration of NO_x, SO_2 and CO analysers, standard gases provided by NRCCRM (National Research Center for Certified Reference Materials, China) were applied. Zero and span checks of all analysers were performed every two days. In addition to the above chemical measurements, key meteorological parameters were monitored by an integrated sensor suite (WXT520, Vaisala, Inc., Finland) including temperature, relative humidity, wind speed, wind direction and precipitation.

2.3 Estimation of site-level OH and NO_3 concentrations by photochemical box model

Since the OH and NO_3 concentrations were not measured in this campaign, they were estimated by using a Photochemical Box Model incorporating Master Chemical Mechanism (PBM-MCM). MCM (v3.2) has a good performance on calculating free radicals and intermediate products (Jenkin et al., 1997;Jenkin et al., 2003;Saunders et al., 2003), as it adopts a near-explicit mechanism, involving 5,900 chemical species and around 16,500 reactions. In this study, the observed hourly data of air pollutants (O_3, NO, NO_2, CO, SO_2 and VOCs) and meteorological parameters (temperature and relative humidity) for the sampling period were input into the model for simulations. More detailed descriptions of the PBM-MCM are provided in Ling et al. (2014), Guo et al. (2013) and Cheng et al. (2010). It is noteworthy that the vertical and horizontal transport and the heterogeneous process of N_2O_5 were not considered in the PBM-MCM. Sensitivity analyses were conducted for the model by varying the mixing ratios of NO_2 and HONO.

2.4 Estimation of regional mixing ratios of daytime OH

Few previous studies have suggested that MCM may not work well for reproducing the OH concentrations in pristine forest environments (Kim et al., 2015). In addition, the OH mixing ratios modelled by the PBM-MCM can only represent the levels at the site. To provide a complement to the PBM-MCM, a widely-used parameterization method using measured aromatic hydrocarbons (*i.e.* BTEX, benzene, toluene, ethylbenzene, and m,p-xylene) was applied to estimate the regional mixing

ratios of daytime OH (Shiu et al., 2007). The ratios of any two aromatics having the same emission sources but different photochemical reactivities can be used to measure photochemical oxidation (Parrish et al., 2007). This approach is based on three assumptions: (1) BTEX are removed from the atmosphere following pseudo-first-order kinetic; (2) no fresh BTEX are emitted to the air mass in the transport, and (3) the effects of horizontal and vertical mixing are similar for each compound. More details about the parameterization method are given in the Text S1.

2.5 Calculation of initial isoprene

To check out the magnitude of isoprene oxidation, the initial isoprene was calculated using a "sequential reaction approach" based on the isoprene's oxidation mechanism and an empirical relationship between isoprene and its first-stage oxidation products (*i.e.* MVK and MACR) (Wolfe et al., 2016). This simplified parameterization method is based on four assumptions: (1) no fresh emissions of isoprene are introduced and isoprene emissions are constant during the process; (2) there were no additional sources of MVK and MACR apart from the oxidation of isoprene; (3) the processing time of the air mass are identical for all three compounds; and (4) only purely chemical reactions are included and the effects of turbulent mixing, horizontal convection and deposition are not accounted for. More description of the calculation is given in the Text S2.

3 Results and Discussion

3.1 Meteorological and chemical conditions

Fig. 2 presents the time series of selected meteorological parameters and trace gases. During the study, the air masses reaching the site were mainly from the southwest and northeast directions. With the change of meteorological conditions, the mixing ratios of air pollutants changed correspondingly. In particular, from Jul 23 to 27, concentrations of anthropogenic pollutants (*i.e.* SO_2, CO and aromatic VOCs) dramatically increased, and were probably affected by regional transport. During Jul 28−31, the relatively higher temperature and lower surface wind enhanced the emissions of isoprene and reduced the dispersion of isoprene and its oxidation products, resulting in the elevated levels of these species in the air. In addition, there was a notable decrease in concentrations of both isoprene and its oxidation products on Aug 2−3 likely caused by continuous rain during the typhoon NIDA. The average temperature was 19.2 ± 0.1 °C (mean ± 95% confidence interval, the same below) and the relative humidity was 92.1 ± 0.6 %. Discontinuities in the figure mean that either no data were available due to the instrumental calibration and maintenance, or the values were below the MDL for those time periods.

Fig. 3 shows the average diurnal patterns of temperature, O_3, NO_2, NO and CO. Time is given in this paper as LST (Local standard time: UTC+8h). During the sampling periods, sunrise and sunset times were about 06:00 and 19:00 LST, respectively. The concentrations of observed O_3, NO_2, NO and CO ranged from 14.4 to 130.6 ppbv (53.5 ± 1.3 ppbv), 0.9 to 10.5 ppbv (2443 ± 74 pptv), 0.6 to 8.7 ppbv (736 ± 37 pptv) and 40.8 to 684.4 ppbv (266.2 ± 6.6 ppbv), respectively. Similar as previous mountaintop studies, a distinct O_3 diurnal variation featured with high levels at night and low levels during the

1 daytime (Zaveri et al., 1995;Gao et al., 2017) was observed in this study, most likely due to a combination of various

2 physical and chemical processes (*e.g.* boundary layer diurnal cycles, mountain-valley breezes, regional transport,

3 photochemical reactions). Since the NO_2 concentrations measured by the molybdenum oxide converter technique can be

4 significantly overestimated in areas far away from fresh NO_x emission sources (Xu et al., 2013), we corrected the observed

5 NO_2 by adopting the hourly modification factors (Fig. S1) obtained at Mount Tai (1,533 m a.s.l.) in central-eastern China

6 (Xu et al., 2013). The modified NO_2 (889 ± 27 pptv) was 1.1−2.5 times (1.8 ± 0.3) lower than that observed. Furthermore,

7 anthropogenic tracers showed very low mixing ratios at this site. For example, the ambient aromatics levels at this site were

8 significantly lower compared to the abundances that measured at a regional background site in the PRD (Wu et al., 2016).

9 Toluene was the most abundant (154 ± 20 pptv), followed by benzene (51 ± 8 pptv), ethylbenzene (47 ± 6 pptv) and m,p-

10 xylene (38 ± 4 pptv).

11 3.2 Isoprene and its oxidation products

12 The hourly averages of isoprene, MVK and MACR were 287 ± 32 pptv (4−2605 pptv), 293 ± 22 pptv (16−1244 pptv), 73 ±

13 6 pptv (10−442 pptv), respectively. Their diurnal behaviours are influenced by a number of chemical (e.g. oxidants levels)

14 and meteorological factors (*e.g.* temperature and sunlight). The hourly averaged daytime isoprene (377 ± 46 pptv, p < 0.01)

15 and MVK (332 ± 32 pptv, p < 0.01) were both higher than the values in nighttime (159 ± 35 pptv and 252 ± 28 pptv,

16 respectively). However, the daytime MACR (66 ± 7 pptv) was slightly lower than its nighttime value (81 ± 10 pptv). In

17 addition, the levels of these compounds decreased substantially at 6 a.m., which could be due to the expansion of the PBL

18 (Fig. S2) and the entrainment of oxidants-rich FT air into the PBL (Vilà-Guerau de Arellano et al., 2011).

19 Table 1 presents the comparison of measurements in this study with previous studies. Surprisingly, the comparison revealed

20 that the isoprene level in this study was much lower than those observed at other sites with similar types of forest, either in

21 China or around the world, particularly if considering a fact that potentially strong isoprene emitters, like evergreen broad-

22 leaved trees and shrubs, are widely seen in this low latitude subtropical-forested region (Bai et al., 2016;Bai et al., 2017).

23 Although the high-altitude feature (1,690 m a.s.l.) may lower the observed isoprene levels as compared with the forest

24 canopy underneath the site, it is still interesting to find that the daytime isoprene concentration (377 ± 46 pptv) in the hottest

25 months of the year (Jul−Aug) was 50%−100% lower than the values observed at the same latitude subtropical-forested sites

26 in Southern China (*e.g.* yearly value of 760 pptv at DingHu Mountain, and summer average of 1,028 pptv at a rural park)

27 (Chen et al., 2010;Wu et al., 2016). Furthermore, O_3 and NO_x levels at this site were generally higher than the observations

28 available in other forest studies worldwide (Table 1). High abundances of O_3 at this site likely indicate strong oxidizing

29 power of the present forest atmospheres. Therefore, these observations may suggest the relevance of the low observed

30 isoprene levels with the complex atmospheric pollution in this region.

31 Isoprene oxidation was the dominant source of MVK and MACR in this remote forest with little transported from

32 anthropogenic sources in neighbor cities at night (see discussion in Text S3), thus the (MVK+MACR)/isoprene ratio can act

1 as an indicator of the isoprene oxidation degree. In this study, the average (MVK+MACR)/isoprene ratio was 4.0 ± 0.8, with

2 the daytime ratio (1.9 ± 0.5, p<0.01) lower than that (6.3 ± 1.4) at night. The daytime ratio in this study was much higher

3 than those reported by previous studies (Table 1). For example, the ratio here is about 5 times higher than that observed at a

4 site 21 m above the canopy reported by Kuhn et al. (2007) in the Amazon rainforest (*i.e.* 0.3 ± 0.1). In addition, studies have

5 also shown that enhanced levels of the (MVK+MACR)/isoprene ratio would be expected in environments where the air mass

6 has aged under high-NOx and high-oxidants conditions (Apel et al., 2002). Therefore, this high (MVK+MACR)/isoprene

7 ratio likely suggests that isoprene was highly oxidized at this site due to strong AOC.

8 ### 3.3 Atmospheric oxidative capacity

9 Above discussions had speculated that the strong AOC might be the main factor contributing to the observed low

10 concentrations of summertime isoprene and high (MVK+MACR)/isoprene ratios at this subtropical forested mountaintop

11 site. Since in this study we did not monitor oxidative radicals with which the analysis of AOC could be more reliable, thus

12 the concentrations of daytime OH and nocturnal NO_3 were modelled by PBM-MCM (Fig. 4).

13 **3.3.1 Daytime OH**

14 The average hourly daytime OH concentration estimated by PBM-MCM at this site was $7.3 ± 0.5 × 10^6$ molecules cm^{-3} (0.36

15 ± 0.03 pptv), with a median value of $7.7 × 10^6$ molecules cm^{-3}. Peaks in concentrations ($14.4 ± 0.8 × 10^6$ molecules cm^{-3})

16 appeared at 12:00 LST when the solar radiation was usually the strongest, and then gradually the concentrations decreased to

17 the lowest levels before sunset. Overall, the calculated OH levels are consistent with the observed values in the PRD (with

18 average and peak value of $~8 × 10^6$ and $1.5–2.6 × 10^7$ molecules cm^{-3}, respectively) (Xiao et al., 2009;Yang et al.,

19 2017;Hofzumahaus et al., 2009). And the range of estimated mixing ratios of daytime OH ($3.6 × 10^5$ to $1.9 × 10^7$ molecules

20 cm^{-3}) in this work generally agrees with the daytime levels ($3.3 × 10^6$ to $2.6 × 10^7$ molecules cm^{-3}) observed at rural sites in

21 the PRD by Xiao et al. (2009), Hofzumahaus et al. (2009) and Lu et al. (2012). The modelled daytime peak OH value is

22 much higher than those observed daytime maxima at remote forest areas such as the Blodgett forest in California ($4 × 10^6$

23 molecules cm^{-3}) (Mao et al., 2012), a boreal forest in Finland ($3.5 × 10^6$ molecules cm^{-3}) (Hens et al., 2014), a pine forest in

24 Alabama ($1 × 10^6$ molecules cm^{-3}) (Feiner et al., 2016) and the Mount Tai in Central China ($5.7 × 10^6$ molecules cm^{-3})

25 (Kanaya et al., 2009). To provide a complement to the PBM-MCM, regional mixing ratios of OH during 9:00-15:00 LST

26 were calculated by a widely-used parameterization method using measured aromatic hydrocarbon ratios, *i.e.* toluene/benzene

27 (T/B), ethylbenzene/benzene (E/B), and m,p-xylene/benzene (X/B) (Fig. S3). The average regional concentrations of OH

28 during 9:00-15:00 LST was $19.7 ± 2.3 × 10^6$ molecules cm^{-3}, even higher than the modelled site-level OH of $11.7 ± 0.4 × 10^6$

29 molecules cm^{-3}. The high concentrations of OH in this study indicate that AOC of this forested region was strong and may

30 facilitate the fast oxidation of daytime isoprene.

3.3.2 Nocturnal NO$_3$

The estimated average nighttime hourly NO$_3$ level was $6.0 \pm 0.5 \times 10^8$ molecules cm^{-3} (29 ± 3 pptv) which is lower than the value obtained at a semi-rural mountain site (~40 pptv) (Sobanski et al., 2016) and at a high-altitude mountain site (~70 pptv) (Chen et al., 2011). The NO$_3$ levels in this study were higher than that (11 pptv) modelled by Guo et al. (2012) and comparable to that (~31 pptv) observed by Brown et al. (2016) both at a mountaintop site (640 m a.s.l.) in Hong Kong. The mixing ratios of NO$_3$ started steady increasing at 7 p.m., peaked at 8 p.m., then rose gradually after midnight, and peaked again at 2 a.m. of the next day. The nocturnal variation of NO$_3$ is similar to that of O$_3$ (peak at 8 p.m.). At the Nanling site, the average nighttime mixing ratios of NO$_2$ (2.5 ± 0.1 ppbv) and O$_3$ (55.5 ± 2.1 ppbv) were relatively high when compared with other remote forest sites (NO$_2$ < 1 ppbv, O$_3$ < 30 ppbv), which provided more favorable conditions for the NO$_3$ formation. In addition, in the surface layer of polluted areas, NO$_3$ is generally low due to the existence of continuously anthropogenic NO as an important NO$_3$ sink; however, in remote or high-altitude mountain regions with cleaner air aloft (*e.g.* in the upper PBL or lower FT), higher NO$_3$ are often observed (Chen et al., 2011;Sobanski et al., 2016;Wang et al., 2017a). The vertical profiles of NO$_3$ obtained by a number of studies have suggested that the NO$_3$ concentration increases with altitude, with a significant fraction existing in the upper PBL or lower FT (Fish et al., 1999;Allan et al., 2002;Friedeburg et al., 2002;Stutz et al., 2004). This is consistent with our results obtained at this high-altitude mountain site. Therefore, the relatively high nighttime NO$_3$ concentrations at this high-altitude mountain site may lead to fast decay of daytime residual isoprene and consequently contribute to MVK and MACR formation.

3.3.3 Uncertainty analysis

Three issues should be noted in applying PBM-MCM to evaluate the AOC in the present study. First, the NO$_2$ concentrations, an important input into PBM-MCM, may be significantly overestimated at this remote mountaintop site that receives a considerable amount of photochemically aged air (Xu et al., 2013). Thus we conducted sensitivity analyses of modelled OH and NO$_3$ with artificially reduced NO$_2$ concentrations for the period Aug 11−Aug 15 2016. The OH and NO$_3$ concentrations decrease with cutting NO$_2$ (Fig. S4). According to a recent study conducted at Mount Tai (Xu et al., 2013), we assumed the daytime and nighttime NO$_2$ measurements were overestimated by 64.4 ± 2.9% and 62.4 ± 3.0%, respectively. Thus the recalculated mean daytime OH concentration would decrease from $7.3 \pm 0.5 \times 10^6$ molecules cm^{-3} to $5.5 \pm 0.4 \times 10^6$ molecules cm^{-3}, with a reduction rate of 23.8 ± 6.2%. And for nighttime NO$_3$, the reduction rate was 41.5 ± 5.2% (from $6.0 \pm 0.5 \times 10^8$ molecules cm^{-3} to $3.5 \pm 0.3 \times 10^8$ molecules cm^{-3}). Second, a number of studies have shown that HONO plays an important role in daytime OH formation (Xue et al., 2014b). As the concentrations of HONO were not measured in the sampling periods, we therefore conducted sensitivity analyses by using a two-day (Aug 13 and Aug 15) dataset coupled with the average diurnal profiles of HONO observed at a background site (Hok Tsui) in Hong Kong in autumn 2012 (Zha, 2015). The results showed that daytime OH concentrations with HONO considered was 22 ± 19% higher than that without HONO (Fig. S5). Finally, the dinitrogen pentoxides (N$_2$O$_5$) that formed from the oxidation of NO$_2$ by NO$_3$ can be taken up onto

aerosols via heterogeneous reactions, which is an important sink of NO_2 and O_3 at night and can compete with the reactions of NO_3 with isoprene (Xue et al., 2014b;Brown et al., 2016;Millet et al., 2016). Unfortunately, we were not able to quantitatively take into account this important mechanism in this study, and further studies are needed to make up this limitation. Overall, current PBM-MCM may have 19 ± 9% and 73 ± 16% overestimation of the daytime OH and nighttime NO_3 concentrations, respectively. Therefore, the PBM-MCM needs improvement and further optimization for its application under the present forested environments.

3.4 Linking observed and initial isoprene

The above discussion kindly suggests the strong AOC might be the main factor contributing to the observed low-level isoprene and high (MVK+MACR)/isoprene ratios in summer. To further confirm this, the initial isoprene which is the total amount of emitted isoprene was calculated. Furthermore, to obtain the oxidation rate of isoprene, the atmospheric reaction time of isoprene can be thereby derived by introducing the estimated concentrations of OH and NO_3.

Initial isoprene was calculated from the observed MVK/isoprene and MACR/isoprene ratios. Fig. 5a shows plots of the initial isoprene versus the observed isoprene (ISO_i/ISO_o) during the day. The initial mixing ratios of daytime isoprene (1213 ± 108 pptv) were much higher than the observed values (377 ± 46 pptv). It is noteworthy that the initial nighttime isoprene by this approach may be overestimated due to the daytime residual MVK and MACR into the night (Fig. S6). The daytime initial mixing ratios of isoprene are 1–40 times of the observed levels, with median and mean values of 2.1 and 4.3, respectively. The ISO_i/ISO_o in this study is comparable with that (ranged from 2 to 40, with a mean value of ~4) obtained at the southeastern US, a photochemistry-active and strong isoprene-emitting region (Wolfe et al., 2016). Scatter plots of calculated initial isoprene versus measured MVK+MACR during daytime hours are also given in Fig. 5b, and a good correlation (R^2=0.71) was obtained. Since the slope is related to the yield of (MVK+MACR) from OH-initiated reaction of isoprene and further oxidation of those two products with OH, data points consistently over the dashed line are likely due to chemical loss of MVK and MACR and/or the influence of continuous emissions of isoprene. These results further confirmed that isoprene was highly oxidized in the air masses, leading to the observed low-level isoprene and high (MVK+MACR)/isoprene ratios.

Fig. 6 shows the derived isoprene reaction times (IRT) from [MVK]/[isoprene] and [MACR]/[isoprene], respectively. IRT derived from the two ratios exhibit a significant linear correlation (R^2=0.91 and 0.90 for daytime and nighttime, respectively). The IRT derived from [MACR]/[isoprene] is 13% lower than that from [MVK]/[isoprene] on average, and we use the mean of these two values. The median and mean IRT during the day is 0.27 and 1.39 hr, respectively, with 4.10 and 4.49 hr at night. The median daytime reaction time (0.27 hr) of measured isoprene was slightly lower than the theoretical lifetime of isoprene (0.40 hr at 12-h daytime averaged [OH] = 8.0×10^6 molecules cm^{-3}). The short reaction time of isoprene indicates fast isoprene oxidation at this mountaintop site.

4 Conclusions

Isoprene and its major intermediate oxidation products MVK and MACR were simultaneously observed in the summer of 2016 at a forested mountaintop site located at the Nanling Mountains in southern China. Although the sampling site was surrounded with subtropical evergreen broad-leaved trees which are strong isoprene emitters, the average daytime isoprene level (377 ± 46 pptv) was found to be significantly lower than other forest studies, while (MVK+MACR)/isoprene ratio (1.9 ± 0.5) and O_3 (51.9 ± 1.7 ppbv) were relatively higher. Based on the observations, we hypothesized that the lower isoprene levels in the study forest might be attributable to a strong AOC in relation to the elevated regional complex air pollution in southern China.

To validate this hypothesis, high daytime OH and nighttime NO_3 radical concentrations were estimated by using a PBM-MCM and a parameterization method. Results from the two approaches are comparable to those observations conducted in the PRD. Although certain uncertainties remained in the present modeling, all radical estimation demonstrated the strong AOC in this subtropical-forested region, which may facilitate fast isoprene oxidation and subsequently contributes to the MVK and MACR formation. In addition, it was found that initial daytime isoprene was 1–40 times of the observed isoprene, with a mean value of 4.3, which are comparable to the photochemistry-active and strong isoprene-emitting southeastern US. Based on the estimated radical concentrations, short daytime atmospheric reaction time (0.27 hr) was subsequently calculated for isoprene during the day. All these indicate that the isoprene was rapidly and highly oxidized over this high-oxidants forest.

To the best of our knowledge, this is the first direct measurements of isoprene and its first-stage oxidation products at this remote, subtropical forested and high-altitude mountain location in southern China. This work highlighted that the air quality and ecological environment of this forest were affected by the highly polluted air from the PRD, particularly the oxidation capacity of the forest′s atmosphere was significantly enhanced. Furthermore, recent long-term observational studies in the PRD (Wang et al., 2009;Xue et al., 2014a;Wang et al., 2017c;Wang et al., 2017b) have indicated the increasing trends of surface O_3, another indicator of the regional AOC. Therefore, continued field observations and further studies are crucial for understanding the relatively high oxidative capacity in this forested region. The feedback of forest ecosystems to the increasing AOC in southern China warrants further studies.

References

Acton, W. J. F., Schallhart, S., Langford, B., Valach, A., Rantala, P., Fares, S., Carriero, G., Tillmann, R., Tomlinson, S. J., Dragosits, U., Gianelle, D., Hewitt, C. N., and Nemitz, E.: Canopy-scale flux measurements and bottom-up emission estimates of volatile organic compounds from a mixed oak and hornbeam forest in northern Italy, Atmos Chem Phys, 16, 7149-7170, 10.5194/acp-16-7149-2016, 2016.

Allan, B. J., Plane, J. M. C., Coe, H., and Shillito, J.: Observations of NO3 concentration profiles in the troposphere, Journal of Geophysical Research: Atmospheres, 107, ACH 11-11-ACH 11-14, 10.1029/2002jd002112, 2002.

Alves, E. G., Jardine, K., Tota, J., Jardine, A., Yanez-Serrano, A. M., Karl, T., Tavares, J., Nelson, B., Gu, D. S., Stavrakou, T., Martin, S., Artaxo, P., Manzi, A., and Guenther, A.: Seasonality of isoprenoid emissions from a primary rainforest in central Amazonia, Atmos Chem Phys, 16, 3903-3925, 10.5194/acp-16-3903-2016, 2016.

Apel, E. C., Riemer, D. D., Hills, A., Baugh, W., Orlando, J., Faloona, I., Tan, D., Brune, W., Lamb, B., Westberg, H., Carroll, M. A., Thornberry, T., and Geron, C. D.: Measurement and interpretation of isoprene fluxes and isoprene, methacrolein, and methyl vinyl ketone mixing ratios at the PROPHET site during the 1998 Intensive, Journal of Geophysical Research-Atmospheres, 107, 15, 10.1029/2000jd000225, 2002.

Bai, J., Guenther, A., Turnipseed, A., Duhl, T., and Greenberg, J.: Seasonal and interannual variations in whole-ecosystem BVOC emissions from a subtropical plantation in China, Atmos Environ, 161, 176-190, 10.1016/j.atmosenv.2017.05.002, 2017.

Bai, J. H., Guenther, A., Turnipseed, A., Duhl, T., Yu, S. Q., and Wang, B.: Seasonal variations in whole-ecosystem BVOC emissions from a subtropical bamboo plantation in China, Atmos Environ, 124, 12-21, 10.1016/j.atmosenv.2015.11.008, 2016.

Brown, S. S., Dube, W. P., Tham, Y. J., Zha, Q. Z., Xue, L. K., Poon, S., Wang, Z., Blake, D. R., Tsui, W., Parrish, D. D., and Wang, T.: Nighttime chemistry at a high altitude site above Hong Kong, Journal of Geophysical Research-Atmospheres, 121, 2457-2475, 10.1002/2015jd024566, 2016.

Chan, C. K., and Yao, X.: Air pollution in mega cities in China, Atmos Environ, 42, 1-42, 10.1016/j.atmosenv.2007.09.003, 2008.

Chen, C. M., Cageao, R. P., Lawrence, L., Stutz, J., Salawitch, R. J., Jourdain, L., Li, Q., and Sander, S. P.: Diurnal variation of midlatitudinal NO3 column abundance over table mountain facility, California, Atmos Chem Phys, 11, 963-978, 10.5194/acp-11-963-2011, 2011.

Chen, H. W., Ho, K. F., Lee, S. C., and Nichol, J. E.: Biogenic volatile organic compounds (BVOC) in ambient air over Hong Kong: analytical methodology and field measurement, International Journal of Environmental Analytical Chemistry, 90, 988-998, 10.1080/03067310903108360, 2010.

Cheng, H. R., Guo, H., Saunders, S. M., Lam, S. H. M., Jiang, F., Wang, X. M., Simpson, I. J., Blake, D. R., Louie, P. K. K., and Wang, T. J.: Assessing photochemical ozone formation in the Pearl River Delta with a photochemical trajectory model, Atmospheric Environment, 44, 4199-4208, 10.1016/j.atmosenv.2010.07.019, 2010.

Claeys, M., Graham, B., Vas, G., Wang, W., Vermeylen, R., Pashynska, V., Cafmeyer, J., Guyon, P., Andreae, M. O., Artaxo, P., and Maenhaut, W.: Formation of secondary organic aerosols through photooxidation of isoprene, Science, 303, 1173-1176, 10.1126/science.1092805, 2004.

Dreyfus, G. B., Schade, G. W., and Goldstein, A. H.: Observational constraints on the contribution of isoprene oxidation to ozone production on the western slope of the Sierra Nevada, California, Journal of Geophysical Research-Atmospheres, 107, 17, 10.1029/2001jd001490, 2002.

Feiner, P. A., Brune, W. H., Miller, D. O., Zhang, L., Cohen, R. C., Romer, P. S., Goldstein, A. H., Keutsch, F. N., Skog, K. M., Wennberg, P. O., Nguyen, T. B., Teng, A. P., DeGouw, J., Koss, A., Wild, R. J., Brown, S. S., Guenther, A., Edgerton, E., Baumann, K., and Fry, J. L.: Testing Atmospheric Oxidation in an Alabama Forest, J Atmos Sci, 73, 4699-4710, 10.1175/Jas-D-16-0044.1, 2016.

Fish, D. J., Shallcross, D. E., and Jones, R. L.: The vertical distribution of NO3 in the atmospheric boundary layer, Atmos Environ, 33, 687-691, 10.1016/S1352-2310(98)00332-X, 1999.

Friedeburg, C. V., Wagner, T., Geyer, A., Kaiser, N., Vogel, B., Vogel, H., and Platt, U.: Derivation of tropospheric NO3 profiles using off‐axis differential optical absorption spectroscopy measurements during sunrise and comparison with simulations, Journal of Geophysical Research, 107, 10.1029/2001JD000481, 2002.

Fuchs, H., Hofzumahaus, A., Rohrer, F., Bohn, B., Brauers, T., Dorn, H. P., Haseler, R., Holland, F., Kaminski, M., Li, X., Lu, K., Nehr, S., Tillmann, R., Wegener, R., and Wahner, A.: Experimental evidence for efficient hydroxyl radical regeneration in isoprene oxidation, Nat Geosci, 6, 1023-1026, 10.1038/Ngeo1964, 2013.

Gao, J., Zhu, B., Xiao, H., Kang, H., Hou, X., Yin, Y., Zhang, L., and Miao, Q.: Diurnal variations and source apportionment of ozone at the summit of Mount Huang, a rural site in Eastern China, Environmental pollution, 222, 513-522, 10.1016/j.envpol.2016.11.031, 2017.

Gu, D., Guenther, A. B., Shilling, J. E., Yu, H., Huang, M., Zhao, C., Yang, Q., Martin, S. T., Artaxo, P., Kim, S., Seco, R., Stavrakou, T., Longo, K. M., Tota, J., de Souza, R. A. F., Vega, O., Liu, Y., Shrivastava, M., Alves, E. G., Santos, F. C., Leng, G., and Hu, Z.: Airborne observations reveal elevational gradient in tropical forest isoprene emissions, Nat Commun, 8, 15541, 10.1038/ncomms15541, 2017.

Guenther, A., Karl, T., Harley, P., Wiedinmyer, C., Palmer, P. I., and Geron, C.: Estimates of global terrestrial isoprene emissions using MEGAN (Model of Emissions of Gases and Aerosols from Nature), Atmos Chem Phys, 6, 3181-3210, DOI 10.5194/acp-6-3181-2006, 2006.

Guenther, A. B., Jiang, X., Heald, C. L., Sakulyanontvittaya, T., Duhl, T., Emmons, L. K., and Wang, X.: The Model of Emissions of Gases and Aerosols from Nature version 2.1 (MEGAN2.1): an extended and updated framework for modeling biogenic emissions, Geoscientific Model Development, 5, 1471-1492, 10.5194/gmd-5-1471-2012, 2012.

Guo, H., Ling, Z. H., Simpson, I. J., Blake, D. R., and Wang, D. W.: Observations of isoprene, methacrolein (MAC) and methyl vinyl ketone (MVK) at a mountain site in Hong Kong, Journal of Geophysical Research-Atmospheres, 117, 13, 10.1029/2012jd017750, 2012.

Guo, H., Ling, Z. H., Cheung, K., Jiang, F., Wang, D. W., Simpson, I. J., Barletta, B., Meinardi, S., Wang, T. J., Wang, X. M., Saunders, S. M., and Blake, D. R.: Characterization of photochemical pollution at different elevations in mountainous areas in Hong Kong, Atmos Chem Phys, 13, 3881-3898, 10.5194/acp-13-3881-2013, 2013.

Hens, K., Novelli, A., Martinez, M., Auld, J., Axinte, R., Bohn, B., Fischer, H., Keronen, P., Kubistin, D., Nolscher, A. C., Oswald, R., Paasonen, P., Petaja, T., Regelin, E., Sander, R., Sinha, V., Sipila, M., Taraborrelli, D., Ernest, C. T., Williams, J., Lelieveld, J., and Harder, H.: Observation and modelling of HOx radicals in a boreal forest, Atmos Chem Phys, 14, 8723-8747, 10.5194/acp-14-8723-2014, 2014.

Hewitt, C. N., Ashworth, K., Boynard, A., Guenther, A., Langford, B., MacKenzie, A. R., Misztal, P. K., Nemitz, E., Owen, S. M., Possell, M., Pugh, T. A. M., Ryan, A. C., and Wild, O.: Ground-level ozone influenced by circadian control of isoprene emissions, Nat Geosci, 4, 671-674, 10.1038/Ngeo1271, 2011.

Hofzumahaus, A., Rohrer, F., Lu, K., Bohn, B., Brauers, T., Chang, C. C., Fuchs, H., Holland, F., Kita, K., Kondo, Y., Li, X., Lou, S., Shao, M., Zeng, L., Wahner, A., and Zhang, Y.: Amplified trace gas removal in the troposphere, Science, 324, 1702-1704, 10.1126/science.1164566, 2009.

Jenkin, M. E., Saunders, S. M., and Pilling, M. J.: The tropospheric degradation of volatile organic compounds: A protocol for mechanism development, Atmospheric Environment, 31, 81-104, 1997.

Jenkin, M. E., Saunders, S. M., Wagner, V., and Pilling, M. J.: Protocol for the development of the Master Chemical Mechanism, MCM v3 (Part B): tropospheric degradation of aromatic volatile organic compounds, Atmos Chem Phys, 3, 181-193, 2003.

Jenkin, M. E., Young, J. C., and Rickard, A. R.: The MCM v3.3.1 degradation scheme for isoprene, Atmos Chem Phys, 15, 11433-11459, 10.5194/acp-15-11433-2015, 2015.

Jones, C. E., Hopkins, J. R., and Lewis, A. C.: In situ measurements of isoprene and monoterpenes within a south-east Asian tropical rainforest, Atmos Chem Phys, 11, 6971-6984, 10.5194/acp-11-6971-2011, 2011.

Kalogridis, C., Gros, V., Sarda-Esteve, R., Langford, B., Loubet, B., Bonsang, B., Bonnaire, N., Nemitz, E., Genard, A. C., Boissard, C., Fernandez, C., Ormeno, E., Baisnee, D., Reiter, I., and Lathiere, J.: Concentrations and fluxes of isoprene and

oxygenated VOCs at a French Mediterranean oak forest, Atmos Chem Phys, 14, 10085-10102, 10.5194/acp-14-10085-2014, 2014.

Kanaya, Y., Pochanart, P., Liu, Y., Li, J., Tanimoto, H., Kato, S., Suthawaree, J., Inomata, S., Taketani, F., Okuzawa, K., Kawamura, K., Akimoto, H., and Wang, Z. F.: Rates and regimes of photochemical ozone production over Central East China in June 2006: a box model analysis using comprehensive measurements of ozone precursors, Atmos Chem Phys, 9, 7711-7723, 10.5194/acp-9-7711-2009, 2009.

Kim, S., Kim, S. Y., Lee, M., Shim, H., Wolfe, G. M., Guenther, A. B., He, A., Hong, Y., and Han, J.: Impact of isoprene and HONO chemistry on ozone and OVOC formation in a semirural South Korean forest, Atmos Chem Phys, 15, 4357-4371, 10.5194/acp-15-4357-2015, 2015.

Kuhn, U., Andreae, M. O., Ammann, C., Araujo, A. C., Brancaleoni, E., Ciccioli, P., Dindorf, T., Frattoni, M., Gatti, L. V., Ganzeveld, L., Kruijt, B., Lelieveld, J., Lloyd, J., Meixner, F. X., Nobre, A. D., Poschl, U., Spirig, C., Stefani, P., Thielmann, A., Valentini, R., and Kesselmeier, J.: Isoprene and monoterpene fluxes from Central Amazonian rainforest inferred from tower-based and airborne measurements, and implications on the atmospheric chemistry and the local carbon budget, Atmos Chem Phys, 7, 2855-2879, 10.5194/acp-7-2855-2007, 2007.

Langford, B., Misztal, P. K., Nemitz, E., Davison, B., Helfter, C., Pugh, T. A. M., MacKenzie, A. R., Lim, S. F., and Hewitt, C. N.: Fluxes and concentrations of volatile organic compounds from a South-East Asian tropical rainforest, Atmos Chem Phys, 10, 8391-8412, 10.5194/acp-10-8391-2010, 2010.

Lelieveld, J., Butler, T. M., Crowley, J. N., Dillon, T. J., Fischer, H., Ganzeveld, L., Harder, H., Lawrence, M. G., Martinez, M., Taraborrelli, D., and Williams, J.: Atmospheric oxidation capacity sustained by a tropical forest, Nature, 452, 737-740, 10.1038/nature06870, 2008.

Li, Z., Xue, L., Yang, X., Zha, Q., Tham, Y. J., Yan, C., Louie, P. K. K., Luk, C. W. Y., Wang, T., and Wang, W.: Oxidizing capacity of the rural atmosphere in Hong Kong, Southern China, The Science of the total environment, 612, 1114-1122, 10.1016/j.scitotenv.2017.08.310, 2018.

Ling, Z. H., Guo, H., Lam, S. H. M., Saunders, S. M., and Wang, T.: Atmospheric photochemical reactivity and ozone production at two sites in Hong Kong: Application of a master chemical mechanism - photochemical box model, Journal of Geophysical Research: Atmospheres, 2014JD021794, 10.1002/2014JD021794, 2014.

Link, M., Zhou, Y., Taubman, B., Sherman, J., Morrow, H., Krintz, I., Robertson, L., Cook, R., Stocks, J., West, M., and Sive, B.: A characterization of volatile organic compounds and secondary organic aerosol at a mountain site in the Southeastern United States, Journal of Atmospheric Chemistry, 72, 81-104, 10.1007/s10874-015-9305-5, 2015.

Liu, Y., Brito, J., Dorris, M. R., Rivera-Rios, J. C., Seco, R., Bates, K. H., Artaxo, P., Duvoisin, S., Jr., Keutsch, F. N., Kim, S., Goldstein, A. H., Guenther, A. B., Manzi, A. O., Souza, R. A., Springston, S. R., Watson, T. B., McKinney, K. A., and Martin, S. T.: Isoprene photochemistry over the Amazon rainforest, Proc Natl Acad Sci U S A, 113, 6125-6130, 10.1073/pnas.1524136113, 2016.

1 Liu, Y., Seco, R., Kim, S., Guenther, A. B., Goldstein, A. H., Keutsch, F. N., Springston, S. R., Watson, T. B., Artaxo, P.,

2 Souza, R. A. F., McKinney, K. A., and Martin, S. T.: Isoprene photo-oxidation products quantify the effect of pollution on

3 hydroxyl radicals over Amazonia, Science Advances, 4, 2018.

4 Lu, K. D., Rohrer, F., Holland, F., Fuchs, H., Bohn, B., Brauers, T., Chang, C. C., Haseler, R., Hu, M., Kita, K., Kondo, Y.,

5 Li, X., Lou, S. R., Nehr, S., Shao, M., Zeng, L. M., Wahner, A., Zhang, Y. H., and Hofzumahaus, A.: Observation and

6 modelling of OH and HO2 concentrations in the Pearl River Delta 2006: a missing OH source in a VOC rich atmosphere,

7 Atmos Chem Phys, 12, 1541-1569, 10.5194/acp-12-1541-2012, 2012.

8 Lu, K. D., Rohrer, F., Holland, F., Fuchs, H., Brauers, T., Oebel, A., Dlugi, R., Hu, M., Li, X., Lou, S. R., Shao, M., Zhu, T.,

9 Wahner, A., Zhang, Y. H., and Hofzumahaus, A.: Nighttime observation and chemistry of HOx in the Pearl River Delta and

10 Beijing in summer 2006, Atmos Chem Phys, 14, 4979-4999, 10.5194/acp-14-4979-2014, 2014.

11 Mao, J., Ren, X., Zhang, L., Van Duin, D. M., Cohen, R. C., Park, J. H., Goldstein, A. H., Paulot, F., Beaver, M. R., Crounse,

12 J. D., Wennberg, P. O., DiGangi, J. P., Henry, S. B., Keutsch, F. N., Park, C., Schade, G. W., Wolfe, G. M., Thornton, J. A.,

13 and Brune, W. H.: Insights into hydroxyl measurements and atmospheric oxidation in a California forest, Atmos Chem Phys,

14 12, 8009-8020, 10.5194/acp-12-8009-2012, 2012.

15 Millet, D. B., Baasandorj, M., Hu, L., Mitroo, D., Turner, J., and Williams, B. J.: Nighttime Chemistry and Morning

16 Isoprene Can Drive Urban Ozone Downwind of a Major Deciduous Forest, Environ Sci Technol, 50, 4335-4342,

17 10.1021/acs.est.5b06367, 2016.

18 Ng, N. L., Brown, S. S., Archibald, A. T., Atlas, E., Cohen, R. C., Crowley, J. N., Day, D. A., Donahue, N. M., Fry, J. L.,

19 Fuchs, H., Griffin, R. J., Guzman, M. I., Herrmann, H., Hodzic, A., Iinuma, Y., Jimenez, J. L., Kiendler-Scharr, A., Lee, B.

20 H., Luecken, D. J., Mao, J. Q., McLaren, R., Mutzel, A., Osthoff, H. D., Ouyang, B., Picquet-Varrault, B., Platt, U., Pye, H.

21 O. T., Rudich, Y., Schwantes, R. H., Shiraiwa, M., Stutz, J., Thornton, J. A., Tilgner, A., Williams, B. J., and Zaveri, R. A.:

22 Nitrate radicals and biogenic volatile organic compounds: oxidation, mechanisms, and organic aerosol, Atmos Chem Phys,

23 17, 2103-2162, 10.5194/acp-17-2103-2017, 2017.

24 Orlando, J. J., and Tyndall, G. S.: Laboratory studies of organic peroxy radical chemistry: an overview with emphasis on

25 recent issues of atmospheric significance, Chem Soc Rev, 41, 6294-6317, 10.1039/c2cs35166h, 2012.

26 Parrish, D. D., Stohl, A., Forster, C., Atlas, E. L., Blake, D. R., Goldan, P. D., Kuster, W. C., and de Gouw, J. A.: Effects of

27 mixing on evolution of hydrocarbon ratios in the troposphere, Journal of Geophysical Research-Atmospheres, 112,

28 10.1029/2006jd007583, 2007.

29 Paulot, F., Crounse, J. D., Kjaergaard, H. G., Kurten, A., St Clair, J. M., Seinfeld, J. H., and Wennberg, P. O.: Unexpected

30 epoxide formation in the gas-phase photooxidation of isoprene, Science, 325, 730-733, 10.1126/science.1172910, 2009.

31 Perring, A. E., Wisthaler, A., Graus, M., Wooldridge, P. J., Lockwood, A. L., Mielke, L. H., Shepson, P. B., Hansel, A., and

32 Cohen, R. C.: A product study of the isoprene+NO3 reaction, Atmos Chem Phys, 9, 4945-4956, 2009.

33 Reissell, A., and Arey, J.: Biogenic volatile organic compounds at Azusa and elevated sites during the 1997 Southern

34 California Ozone Study, Journal of Geophysical Research-Atmospheres, 106, 1607-1621, Doi 10.1029/2000jd900517, 2001.

1　Rhew, R. C., Deventer, M. J., Turnipseed, A. A., Warneke, C., Ortega, J., Shen, S., Martinez, L., Koss, A., Lerner, B. M.,

2　Gilman, J. B., Smith, J. N., Guenther, A. B., and de Gouw, J. A.: Ethene, propene, butene and isoprene emissions from a

3　ponderosa pine forest measured by relaxed eddy accumulation, Atmos Chem Phys, 17, 13417-13438, 10.5194/acp-17-

4　13417-2017, 2017.

5　Rohrer, F., Lu, K. D., Hofzumahaus, A., Bohn, B., Brauers, T., Chang, C. C., Fuchs, H., Haseler, R., Holland, F., Hu, M.,

6　Kita, K., Kondo, Y., Li, X., Lou, S. R., Oebel, A., Shao, M., Zeng, L. M., Zhu, T., Zhang, Y. H., and Wahner, A.: Maximum

7　efficiency in the hydroxyl-radical-based self-cleansing of the troposphere, Nat Geosci, 7, 559-563, 10.1038/Ngeo2199, 2014.

8　Santos, F., Longo, K., Guenther, A., Kim, S., Gu, D., Oram, D., Forster, G., Lee, J., Hopkins, J., Brito, J., and Freitas, S.:

9　Biomass burning emission disturbances of isoprene oxidation in a tropical forest, Atmos Chem Phys, 18, 12715-12734,

10　10.5194/acp-18-12715-2018, 2018.

11　Saunders, S. M., Jenkin, M. E., Derwent, R. G., and Pilling, M. J.: Protocol for the development of the Master Chemical

12　Mechanism, MCM v3 (Part A): tropospheric degradation of non-aromatic volatile organic compounds, Atmos Chem Phys, 3,

13　161-180, 2003.

14　Seco, R., Penuelas, J., Filella, I., Llusia, J., Molowny-Horas, R., Schallhart, S., Metzger, A., Muller, M., and Hansel, A.:

15　Contrasting winter and summer VOC mixing ratios at a forest site in the Western Mediterranean Basin: the effect of local

16　biogenic emissions, Atmos Chem Phys, 11, 13161-13179, 10.5194/acp-11-13161-2011, 2011.

17　SFAPRC: Statistics of Forest Resources in China (2009-2013): The 8th national forest inventory. State Forestry

18　Administration, P.R. China. (in Chinese), China Forestry Publishing House, 2014.

19　Shiu, C. J., Liu, S. C., Chang, C. C., Chen, J. P., Chou, C. C. K., Lin, C. Y., and Young, C. Y.: Photochemical production of

20　ozone and control strategy for Southern Taiwan, Atmos Environ, 41, 9324-9340, 10.1016/j.atmosenv.2007.09.014, 2007.

21　Sobanski, N., Tang, M. J., Thieser, J., Schuster, G., Pohler, D., Fischer, H., Song, W., Sauvage, C., Williams, J., Fachinger,

22　J., Berkes, F., Hoor, P., Platt, U., Lelieveld, J., and Crowley, J. N.: Chemical and meteorological influences on the lifetime of

23　NO3 at a semi-rural mountain site during PARADE, Atmos Chem Phys, 16, 4867-4883, 10.5194/acp-16-4867-2016, 2016.

24　Sprengnether, M., Demerjian, K. L., Donahue, N. M., and Anderson, J. G.: Product analysis of the OH oxidation of isoprene

25　and 1,3-butadiene in the presence of NO, Journal of Geophysical Research: Atmospheres, 107, ACH 8-1-ACH 8-13,

26　10.1029/2001JD000716, 2002.

27　Stroud, C. A., Roberts, J. M., Goldan, P. D., Kuster, W. C., Murphy, P. C., Williams, E. J., Hereid, D., Parrish, D., Sueper,

28　D., Trainer, M., Fehsenfeld, F. C., Apel, E. C., Riemer, D., Wert, B., Henry, B., Fried, A., Martinez-Harder, M., Harder, H.,

29　Brune, W. H., Li, G., Xie, H., and Young, V. L.: Isoprene and its oxidation products, methacrolein and methylvinyl ketone,

30　at an urban forested site during the 1999 Southern Oxidants Study, Journal of Geophysical Research-Atmospheres, 106,

31　8035-8046, Doi 10.1029/2000jd900628, 2001.

32　Stutz, J., Alicke, B., Ackermann, R., Geyer, A., White, A. B., and Williams, E. J.: Vertical profiles of NO3, N2O5, O3, and

33　NOx in the nocturnal boundary layer: 1. Observations during the Texas Air Quality Study 2000, Journal of Geophysical

34　Research, 109, 10.1029/2004JD005216, 2004.

Su, L. P., Patton, E. G., de Arellano, J. V. G., Guenther, A. B., Kaser, L., Yuan, B., Xiong, F. L. Z., Shepson, P. B., Zhang, L., Miller, D. O., Brune, W. H., Baumann, K., Edgerton, E., Weinheimer, A., Misztal, P. K., Park, J. H., Goldstein, A. H., Skog, K. M., Keutsch, F. N., and Mak, J. E.: Understanding isoprene photooxidation using observations and modeling over a subtropical forest in the southeastern US, Atmos Chem Phys, 16, 7725-7741, 10.5194/acp-16-7725-2016, 2016.

Tang, J. H., Chan, L. Y., Chang, C. C., Liu, S., and Li, Y. S.: Characteristics and sources of non-methane hydrocarbons in background atmospheres of eastern, southwestern, and southern China, Journal of Geophysical Research-Atmospheres, 114, 10.1029/2008jd010333, 2009.

Taraborrelli, D., Lawrence, M. G., Crowley, J. N., Dillon, T. J., Gromov, S., Groß, C. B. M., Vereecken, L., and Lelieveld, J.: Hydroxyl radical buffered by isoprene oxidation over tropical forests, Nat Geosci, 5, 190-193, 10.1038/ngeo1405, 2012.

Thomas D Sharkey, and Yeh, S.: Isoprene emission from plants, Annual Review of Plant Biology, 52, 407, 2003.

Vilà-Guerau de Arellano, J., Patton, E. G., Karl, T., van den Dries, K., Barth, M. C., and Orlando, J. J.: The role of boundary layer dynamics on the diurnal evolution of isoprene and the hydroxyl radical over tropical forests, Journal of Geophysical Research, 116, 10.1029/2010jd014857, 2011.

Wang, H. C., Lu, K. D., Tan, Z. F., Sun, K., Li, X., Hu, M., Shao, M., Zeng, L. M., Zhu, T., and Zhang, Y. H.: Model simulation of NO3, N2O5 and ClNO2 at a rural site in Beijing during CAREBeijing-2006, Atmos Res, 196, 97-107, 10.1016/j.atmosres.2017.06.013, 2017a.

Wang, M., Zeng, L. M., Lu, S. H., Shao, M., Liu, X. L., Yu, X. N., Chen, W. T., Yuan, B., Zhang, Q., Hu, M., and Zhang, Z. Y.: Development and validation of a cryogen-free automatic gas chromatograph system (GC-MS/FID) for online measurements of volatile organic compounds, Analytical Methods, 6, 9424-9434, 10.1039/c4ay01855a, 2014.

Wang, T., Guo, H., Blake, D. R., Kwok, Y. H., Simpson, I. J., and Li, Y. S.: Measurements of trace gases in the inflow of South China Sea background air and outflow of regional pollution at Tai O, Southern China, Journal of Atmospheric Chemistry, 52, 295-317, 10.1007/s10874-005-2219-x, 2005.

Wang, T., Wei, X. L., Ding, A. J., Poon, C. N., Lam, K. S., Li, Y. S., Chan, L. Y., and Anson, M.: Increasing surface ozone concentrations in the background atmosphere of Southern China, 1994-2007, Atmos Chem Phys, 9, 6217-6227, 2009.

Wang, T., Xue, L., Brimblecombe, P., Lam, Y. F., Li, L., and Zhang, L.: Ozone pollution in China: A review of concentrations, meteorological influences, chemical precursors, and effects, The Science of the total environment, 575, 1582-1596, 10.1016/j.scitotenv.2016.10.081, 2017b.

Wang, Y., Wang, H., Guo, H., Lyu, X., Cheng, H., Ling, Z., Louie, P. K. K., Simpson, I. J., Meinardi, S., and Blake, D. R.: Long term O3-precursor relationships in Hong Kong: Field observation and model simulation, Atmospheric Chemistry and Physics Discussions, 1-29, 10.5194/acp-2017-235, 2017c.

Wayne, R. P., Barnes, I., Biggs, P., Burrows, J. P., Canosamas, C. E., Hjorth, J., Bras, G. L., Moortgat, G. K., Perner, D., and Poulet, G. J. A. E. P. A. G. T.: The Nitrate Radical: Physics, Chemistry and the Atmosphere, 25, 1-203, 1991.

Wolfe, G. M., Kaiser, J., Hanisco, T. F., Keutsch, F. N., de Gouw, J. A., Gilman, J. B., Graus, M., Hatch, C. D., Holloway, J., Horowitz, L. W., Lee, B. H., Lerner, B. M., Lopez-Hilifiker, F., Mao, J., Marvin, M. R., Peischl, J., Pollack, I. B., Roberts, J.

M., Ryerson, T. B., Thornton, J. A., Veres, P. R., and Warneke, C.: Formaldehyde production from isoprene oxidation across NOx regimes, Atmos Chem Phys, 16, 2597-2610, 10.5194/acp-16-2597-2016, 2016.

Wu, F., Yu, Y., Sun, J., Zhang, J., Wang, J., Tang, G., and Wang, Y.: Characteristics, source apportionment and reactivity of ambient volatile organic compounds at Dinghu Mountain in Guangdong Province, China, The Science of the total environment, 548-549, 347-359, 10.1016/j.scitotenv.2015.11.069, 2016.

Wu, M., Wu, D., Fan, Q., Wang, B. M., Li, H. W., and Fan, S. J.: Observational studies of the meteorological characteristics associated with poor air quality over the Pearl River Delta in China, Atmos Chem Phys, 13, 10755-10766, 10.5194/acp-13-10755-2013, 2013.

Xiao, R., Takegawa, N., Kondo, Y., Miyazaki, Y., Miyakawa, T., Hu, M., Shao, M., Zeng, L. M., Hofzumahaus, A., Holland, F., Lu, K., Sugimoto, N., Zhao, Y., and Zhang, Y. H.: Formation of submicron sulfate and organic aerosols in the outflow from the urban region of the Pearl River Delta in China, Atmos Environ, 43, 3754-3763, 10.1016/j.atmosenv.2009.04.028, 2009.

Xu, Z., Wang, T., Xue, L. K., Louie, P. K. K., Luk, C. W. Y., Gao, J., Wang, S. L., Chai, F. H., and Wang, W. X.: Evaluating the uncertainties of thermal catalytic conversion in measuring atmospheric nitrogen dioxide at four differently polluted sites in China, Atmos Environ, 76, 221-226, 10.1016/j.atmosenv.2012.09.043, 2013.

Xue, L., Wang, T., Louie, P. K., Luk, C. W., Blake, D. R., and Xu, Z.: Increasing external effects negate local efforts to control ozone air pollution: a case study of Hong Kong and implications for other Chinese cities, Environ Sci Technol, 48, 10769-10775, 10.1021/es503278g, 2014a.

Xue, L. K., Wang, T., Guo, H., Blake, D. R., Tang, J., Zhang, X. C., Saunders, S. M., and Wang, W. X.: Sources and photochemistry of volatile organic compounds in the remote atmosphere of western China: results from the Mt. Waliguan Observatory, Atmos Chem Phys, 13, 8551-8567, 10.5194/acp-13-8551-2013, 2013.

Xue, L. K., Wang, T., Gao, J., Ding, A. J., Zhou, X. H., Blake, D. R., Wang, X. F., Saunders, S. M., Fan, S. J., Zuo, H. C., Zhang, Q. Z., and Wang, W. X.: Ground-level ozone in four Chinese cities: precursors, regional transport and heterogeneous processes, Atmos. Chem. Phys., 14, 13175-13188, 10.5194/acp-14-13175-2014, 2014b.

Xue, L. K., Gu, R. R., Wang, T., Wang, X. F., Saunders, S., Blake, D., Louie, P. K. K., Luk, C. W. Y., Simpson, I., Xu, Z., Wang, Z., Gao, Y., Lee, S. C., Mellouki, A., and Wang, W. X.: Oxidative capacity and radical chemistry in the polluted atmosphere of Hong Kong and Pearl River Delta region: analysis of a severe photochemical smog episode, Atmos Chem Phys, 16, 9891-9903, 10.5194/acp-16-9891-2016, 2016.

Yang, Y. D., Shao, M., Kessel, S., Li, Y., Lu, K. D., Lu, S. H., Williams, J., Zhang, Y. H., Zeng, L. M., Noelscher, A. C., Wu, Y. S., Wang, X. M., and Zheng, J. Y.: How the OH reactivity affects the ozone production efficiency: case studies in Beijing and Heshan, China, Atmos Chem Phys, 17, 7127-7142, 10.5194/acp-17-7127-2017, 2017.

Zaveri, R. A., Saylor, R. D., Peters, L. K., McNider, R., and SonG, A.: A model investigation of summertime diurnal ozone behaviour in rural mountainous locations, Atmos Environ, 29, 1043-1065, 1995.

1 Zha, Q.: Measurement of nitrous acid (HONO) and the implications to photochemical pollution, MPhil dissertation,
2 Department of Civil and Environmental Engineering, The Hong Kong Polytechnic University, 2015.

3 Zheng, J. Y., Zhong, L. J., Wang, T., Louie, P. K. K., and Li, Z. C.: Ground-level ozone in the Pearl River Delta region:
4 Analysis of data from a recently established regional air quality monitoring network, Atmos Environ, 44, 814-823,
5 10.1016/j.atmosenv.2009.11.032, 2010.

6 Zhu, Y., Yang, L., Kawamura, K., Chen, J., Ono, K., Wang, X., Xue, L., and Wang, W.: Contributions and source
7 identification of biogenic and anthropogenic hydrocarbons to secondary organic aerosols at Mt. Tai in 2014, Environmental
8 pollution, 220, 863-872, 10.1016/j.envpol.2016.10.070, 2017.

9

Tables

Table 1: Comparison of average concentrations (in ppbv, mean ± 1σ standard deviation or 95% confidence interval) of isoprene, O$_3$, NO$_2$ and NO measured at the Nanling site, as well as (MVK+MACR)/isoprene ratios (ppbv/ppbv) and altitude (m a.s.l.), with other forest or mountaintop sites.

Forest type and latitude	Altitude	Isoprene	Ratio [a]	O$_3$, NO$_2$, NO [b]	Sampling time	References
Subtropical (24.70° N)	1690	0.377 ±0.046	1.9±0.5	51.9±1.7, 2.39±0.11, 0.80±0.06	Daytime (summer)	
		0.159±0.035	6.3±1.4	55.5±2.1, 2.51±0.10, 0.66±0.05	Nighttime (summer)	This study
		0.287±0.032	4.0±0.8	53.5±1.3, 2.44±0.07, 0.74±0.04	Daily (summer)	
Subtropical (23.17° N)	1000	0.76±0.50	- [c]	-	Daytime (all year)	Wu et al. (2016)
Subtropical (22.29° N)	507	1.028±0.025	-	-	Daytime (summer)	Chen et al. (2010)
Subtropical (30.50° N)	130	0.39±0.27	-	-	Daytime (spring)	Tang et al. (2009)
Tropical (18.67° N)	820	0.55±0.52	-	-	Daytime (wet season)	Tang et al. (2009)
Deciduous (22.25° N)	80	0.370±0.157	-	42±22, -, 2.4±3.6	Daytime (all year)	Wang et al. (2005)
Mt. Tai (36.25° N)	1533	0.15±0.18	-	-	Daily (summer)	Zhu et al. (2017)
Tibet (36.3° N)	3816	0.126±0.287	-	54±11, 3.60±1.13 [c], 0.05±0.03	Daily (summer)	Xue et al. (2013)
Temperate (45.56° N)	801	1.90 ± 0.43	0.4	-, 1.0, 0.1	Midday (summer)	Apel et al. (2002)
Ponderosa (39.1° N)	2840	0.148 ± 0.098	-	-	Daily (summer)	Rhew et al. (2017)
Deciduous (36.21° N)	1100	0.743±0.575	0.6	-	Daily (summer)	Link et al. (2015)
Deciduous (43.93° N)	650	1.19	0.13±0.05	-, <3, <0.2	Daily (summer)	Kalogridis et al. (2014)
Deciduous (45.20° N)	24	1.07±0.80	0.5	-	Daily (summer)	Acton et al. (2016)
Coniferous (38.90° N)	1315	0.397±0.558	-	-	Daily (summer)	Dreyfus et al. (2002)
Mediterranean (41.78° N)	720	0.43	0.7	37.5, 1.0, 0.8	Daily (summer)	Seco et al. (2011)
Tropical (4.98° N)	426	1.4±1.2	<0.4	-	Daily (dry season)	Langford et al. (2010)
Tropical (4.98° N)	426	1.058	0.5	-	Daily (wet season)	Jones et al. (2011)
Tropical (2.59° S)	103	1.66±0.90	-	-	Daytime (wet season)	Alves et al. (2016)
Tropical (2.59° S)	103	3.4	0.31±0.07	15.0, -, -	Daytime (dry season)	Kuhn et al. (2007)

[a] Represent the (MVK+MACR)/isoprene ratio. [b] Observed data. [c] Data not reported or not applicable. [d] NO$_y$.
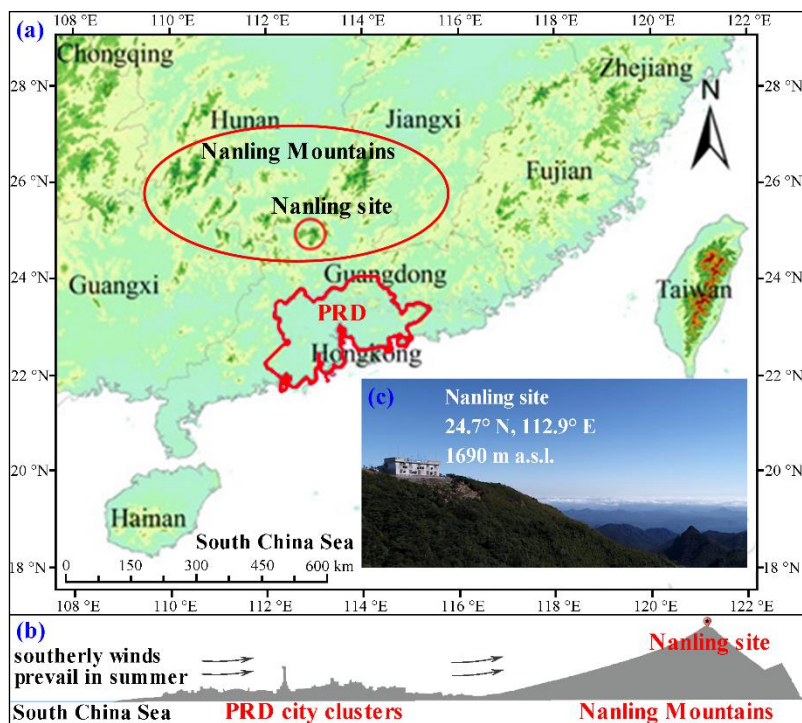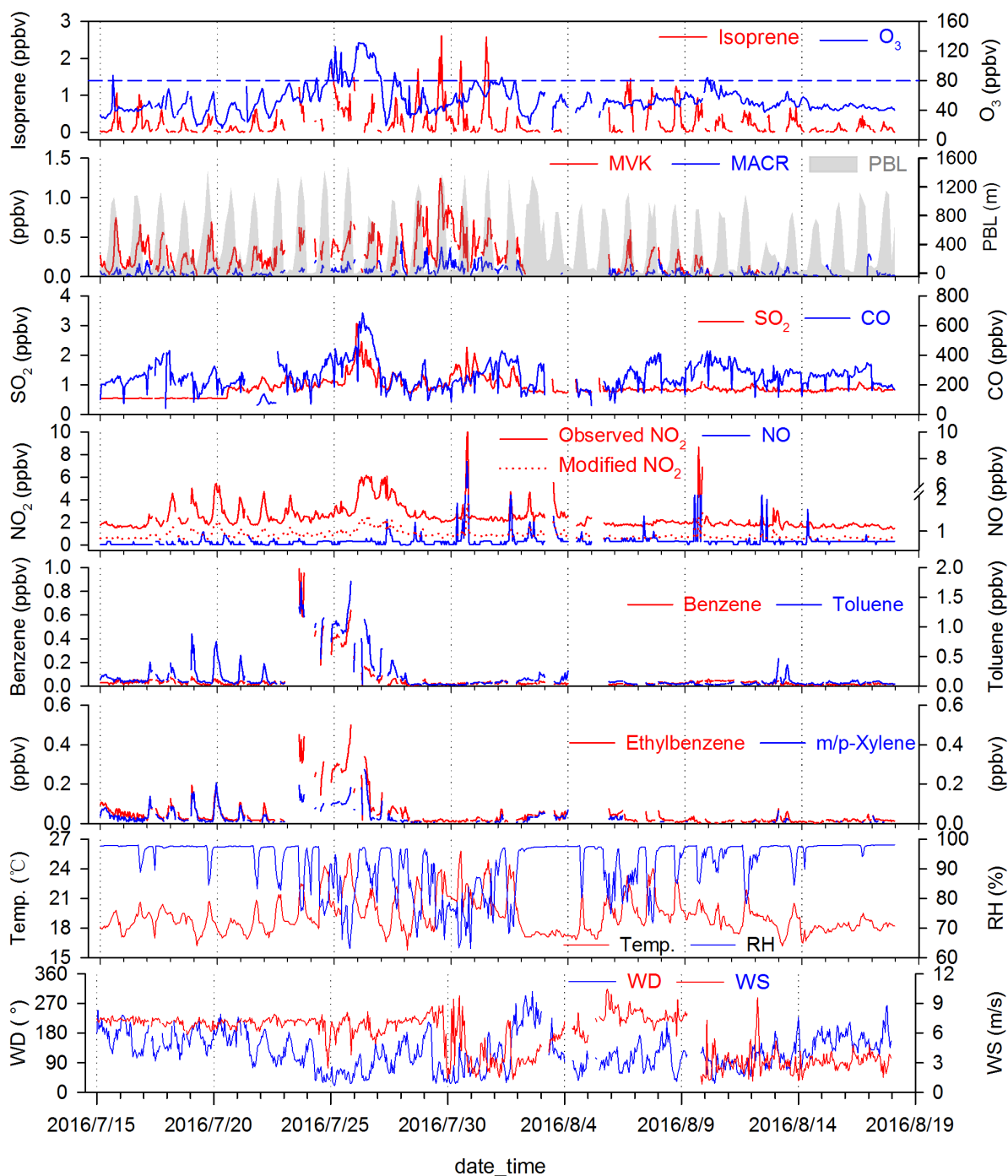
2

3 **Fig. 1: (a) Map showing the location of the Nanling site at the summit of Mt. Tian Jing in southern Nanling Mountains; (b) Also**
4 **shown is the sketch of cross-section of the PRD and Nanling Mountains; (c) Aerial photo of the Nanling site. The base map in Fig.**
5 **1a and Fig.1b are reproduced from Wu et al. (2016) and Wu et al. (2013), respectively.**

6

1

2 **Fig. 2**: Time series (1-hour data) of trace gases, meteorological parameters and **Planetary Boundary Layer (PBL)**height (**PBL** data
3 provided by Real-time Environmental Applications and Display System, https://ready.arl.noaa.gov/READYamet.php) during Jul
4 15–Aug 17 2016 at the Nanling site. Modified NO_2 defined here as the product of modification factor (Fig. S1) and observed NO_2.
5 Blue dashed lines are Grade I of the Ambient Air Quality Standard in China for O_3 (80 ppbv). Temperature, relative humidity,
6 wind speed and wind direction are referred to as Temp., RH, WS and WD, respectively.

1

2
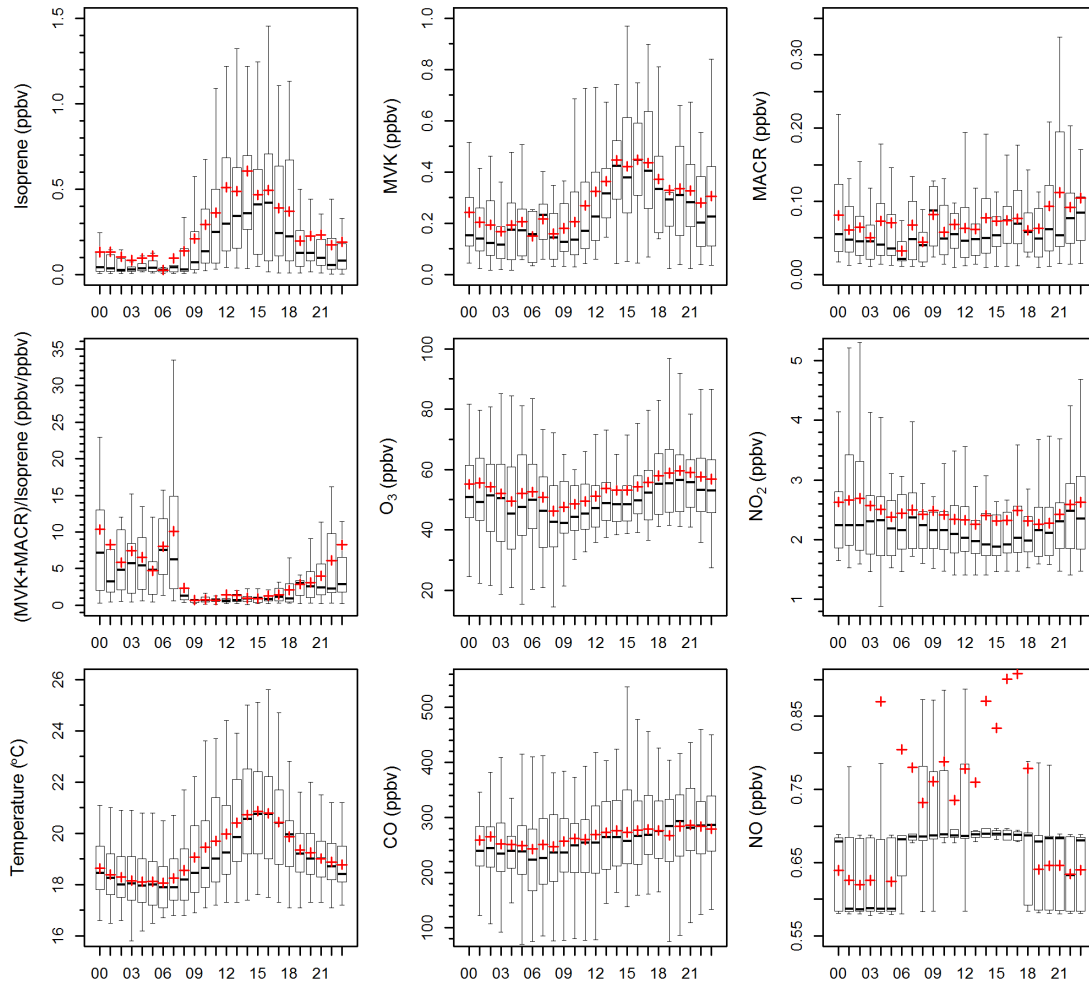
Fig. 3: Box and whisker plots of average diurnal patterns of observed isoprene, MVK, MACR, (MVK+MACR)/isoprene ratios, O_3, NO_2, temperature, CO and NO. The X-axis is "hour of day". The black thick line and red plus sign represent the median and mean value, respectively.

6

25

1
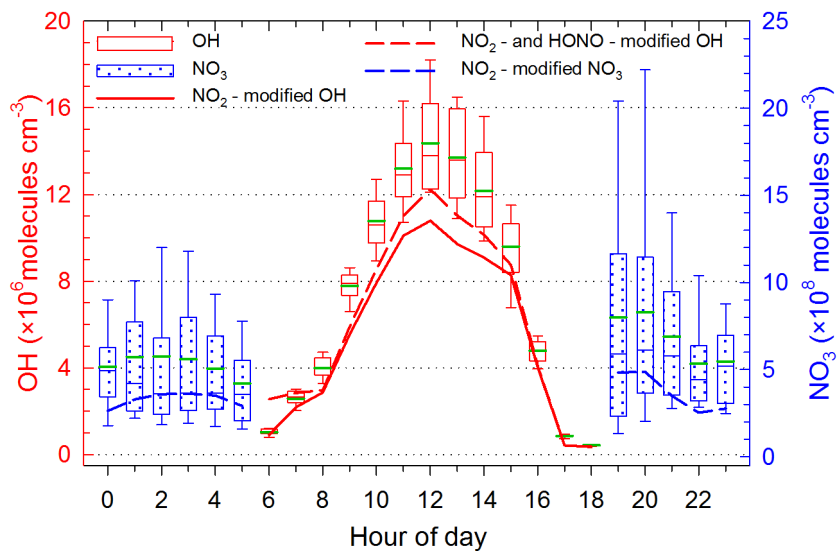
Fig. 4: Box and whisker plots of average diurnal patterns of PBM-MCM modelled OH and NO_3 concentrations. The green thick
line represents the mean value. Also shown are the results after conducting sensitivity analyses for the model by modifying the
mixing ratios of NO_2 and HONO.
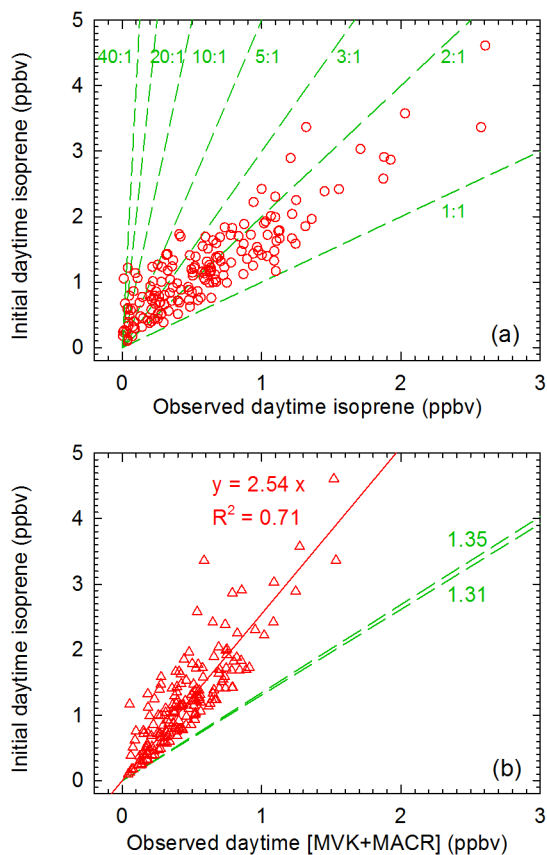
1

2 **Fig. 5**: **(a) Comparison of observed and initial isoprene mixing ratios during the day. Green dashed lines denote slopes for different**
3 **ratios of initial to observed isoprene. (b) Relationship between initial isoprene and observed [MVK+MACR] during the day. The**
4 **green dashed lines denote slopes for different yields of (MVK+MACR) of the OH-initiated oxidation of isoprene for the ranges of**
5 **the observed NO distribution (Fig. S7).**

6
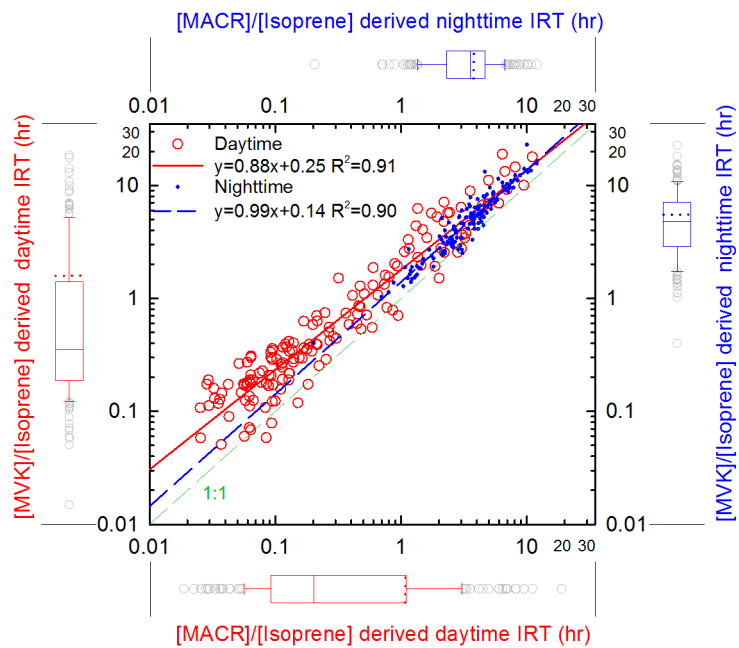
Fig. 6: Isoprene reaction time (IRT) derived from [MVK]/[isoprene] and [MACR]/[isoprene] based on the modelled OH and NO_3 concentrations. The green dashed line denotes a 1:1 relationship. Next to axes are the box and whisker plots of each result, and the dotted lines denote the mean values.

Supplement of

Low-level summertime isoprene observed at a forested mountaintop site in southern China: Implications for strong regional atmospheric oxidative capacity

Daocheng Gong and Hao Wang et al.

Correspondence to:

Boguang Wang (tbongue@jnu.edu.cn)

Text S1. **Estimation of regional mixing ratios of daytime OH**

It is well known that BTEX (benzene, toluene, ethylbenzene, and m,p-xylene) are the most important aromatic hydrocarbons regarding their universal anthropogenic sources. Because of their atmospheric lifetimes of up to several days (Table S1), BTEX can undergo long-range transport. The ratio of two aromatics that share common emission sources but with different reactivities with hydroxyl radical (OH) can be used as a measure of photochemical oxidation by OH (Parrish et al., 2007;Shiu et al., 2007). Thus, BTEX provide particularly promising capabilities for following photochemical processing on timescales of hours to days. In this study, we chose three pairs of aromatic species: toluene/benzene, ethylbenzene/benzene, and m,p-xylene/benzene.

During daytime, decreasing of BTEX levels along transport path owes mainly to atmospheric dilution and reaction with OH. The chemical removal of BTEX by OH can be expressed as followings:

$Benzene + OH \rightarrow$ products $\qquad k_{benzene,OH} = 2.3 \times 10^{-12} \, e^{-190/T}$ $\qquad\qquad$ (R1)

$Toluene + OH \rightarrow$ products $\qquad k_{Toluene,OH} = 1.8 \times 10^{-12} \, e^{340/T}$ $\qquad\qquad$ (R2)

$Ethylbenzene + OH \rightarrow$ products $\quad k_{Ethylbenzene,OH} = 7.0 \times 10^{-12}$ $\qquad\qquad$ (R3)

$m, p - Xylene + OH \rightarrow$ products $\quad k_{m,p-Xylene,OH} = 1.89 \times 10^{-11}$ $\qquad\qquad$ (R4)
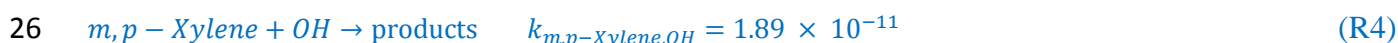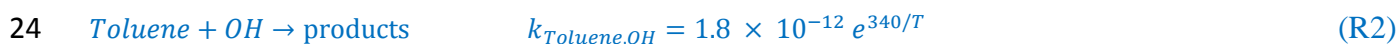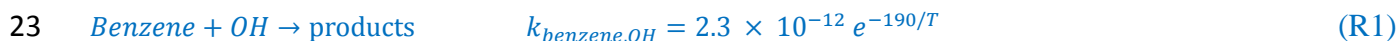
Thus, mixing ratios of BTEX at the sampling time can be expressed as follows, for example, in the case of benzene,

1    $$[B]_t = [B]_0 \times e^{-[OH] \times k_{B,OH} \times t} \times f_{d,B} \tag{Eq.1}$$

2   where $[B]_0$ and $[B]_t$ represents the mixing ratios of measured benzene at the start and after transport time t

3   that air mass spent in the atmosphere, respectively. $k_{B,OH}$ represents the temperature dependent reaction rate

4   coefficient of benzene with OH, which was taken from the IUPAC database (http://iupac.pole-ether.fr/)

5   (Atkinson et al., 2006). $[OH]$ represents the regional concentrations of OH. $f_{d,B}$ represents the dilution factor

6   of benzene in the atmosphere.

7   Toluene, ethylbenzene and m,p-xylene react faster with OH than benzene. In this study, we assuming the

8   rates of turbulent mixing and horizontal convection are similar for BTEX. Therefore, during the transport

9   time Δt, the dilution factor of BTEX are the same. Then rearranging Eq.1 and extending this analysis to

10   BTEX will yield the following equations.

11    $$[OH]_{T/B} = \frac{1}{t \times (k_{T,OH} - k_{B,OH})} \times \left[\ln\left(\frac{[T]}{[B]}\right)_0 - \ln\left(\frac{[T]}{[B]}\right)_t \right] \tag{Eq.2}$$

12    $$[OH]_{E/B} = \frac{1}{t \times (k_{E,OH} - k_{B,OH})} \times \left[\ln\left(\frac{[E]}{[B]}\right)_0 - \ln\left(\frac{[E]}{[B]}\right)_t \right] \tag{Eq.3}$$

13    $$[OH]_{X/B} = \frac{1}{t \times (k_{X,OH} - k_{B,OH})} \times \left[\ln\left(\frac{[X]}{[B]}\right)_0 - \ln\left(\frac{[X]}{[B]}\right)_t \right] \tag{Eq.4}$$

14   Where $[OH]_{T/B}$, $[OH]_{E/B}$, and $[OH]_{X/B}$ represent the estimated regional mixing ratios of OH by three

15   aromatic ratios. It should be noted that the data included only daytime observations between 09:00–15:00

16   LST when the aromatic ratios presented a smoothly decreasing trend (Fig. S3). In addition, the X/B ratio

17   may not work well in comparison with T/B and E/B owing to the relatively short lifetime of m,p-xylene

18   (Table S1). Indeed, results derived from X/B are significantly lower than those from T/B and E/B, and we

19   use the mean values derived by T/B and E/B in this study. The scatterplots of the regional mixing ratios of

20   OH derived from the three ratios were presented in the Fig. S8, and the diurnal patterns were presented in

21   the Fig. S9.

22   **Text S2.** **Calculation of initial isoprene**

23   The first-stage oxidation of isoprene (ISO), MVK and MACR by reaction with OH during the day, and with

24   NO$_3$ at night, can be described by the following reactions:

25    $ISO + OH \rightarrow y_{MACR,OH}\, MACR + y_{MVK,OH}\, MVK$ $k_{ISO,OH} = 2.7 \times 10^{-11}\, e^{390/T}$ (R5)

26    $MVK + OH \rightarrow products$ $k_{MVK,OH} = 2.6 \times 10^{-12}\, e^{610/T}$ (R6)

27    $MACR + OH \rightarrow$ products $k_{MACR,OH} = 8.0 \times 10^{-12}\, e^{380/T}$ (R7)

28    $ISO + NO_3 \rightarrow y_{MACR,NO_3}\, MACR + y_{MVK,NO_3}\, MVK$ $k_{ISO,NO_3} = 2.95 \times 10^{-12}\, e^{-450/T}$ (R8)
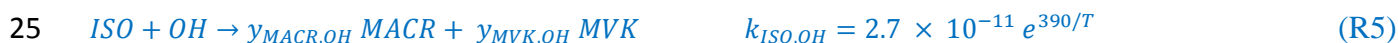
1    $MVK + NO_3 \rightarrow$ products $k_{MVK,NO_3} < 6.0 \times 10^{-16}$ (R9)

2    $MACR + NO_3 \rightarrow$ products $k_{MACR,NO_3} = 3.4 \times 10^{-15}$ (R10)

3   Where k is the temperature dependent reaction rate coefficients taken from the IUPAC database

4   (http://iupac.pole-ether.fr/) (Atkinson et al., 2006). y are yields of MVK and MACR from isoprene reaction

5   with OH and NO₃. T is the temperature (unit in K).

6   Then, the product/parent ratios, *i.e.* [MVK]/[ISO] and [MVK]/[ISO], can be calculated as a function of the

7   rate constants (k), yield (y), reaction time (Δt) and radical concentration ([OH] and [NO_3]):

8    $\left(\frac{[MVK]}{[ISO]}\right)_D = \frac{y_{MVK,OH}\, k_{ISO,OH}}{(k_{MVK,OH}-k_{ISO,OH})} \times \left[1 - e^{(k_{ISO,OH}-k_{MVK,OH})\,[OH]\,\Delta t}\right]$ (Eq.5)

9    $\left(\frac{[MACR]}{[ISO]}\right)_D = \frac{y_{MACR,OH}\, k_{ISO,OH}}{(k_{MACR,OH}-k_{ISO,OH})} \times \left[1 - e^{(k_{ISO,OH}-k_{MACR,OH})\,[OH]\,\Delta t}\right]$ (Eq.6)

10    $\left(\frac{[MVK]}{[ISO]}\right)_N = \frac{y_{MVK,NO_3}\, k_{ISO,NO_3}}{(k_{MVK,NO_3}-k_{ISO,NO_3})} \times \left[1 - e^{(k_{ISO,NO_3}-k_{MVK,NO_3})\,[NO_3]\,\Delta t}\right]$ (Eq.7)

11    $\left(\frac{[MACR]}{[ISO]}\right)_N = \frac{y_{MACR,NO_3}\, k_{ISO,NO_3}}{(k_{MACR,NO_3}-k_{ISO,NO_3})} \times \left[1 - e^{(k_{ISO,NO_3}-k_{MACR,NO_3})\,[NO_3]\,\Delta t}\right]$ (Eq.8)

12   Where [ISO], [MVK] and [$MACR$] represent the observed isoprene, MVK and MACR. [OH] and [NO_3]

13   represent daytime OH and nighttime NO₃, respectively. D and N represent daytime and nighttime periods,

14   respectively. Δt is the atmospheric reaction time of isoprene, representing the time of isoprene in the

15   atmosphere between emission and detection.

16   Initial isoprene [ISO]$_i$, the total isoprene emissions that have been released into the sample air masses, can

17   be effectively calculated via reverse integration of isoprene's first-stage oxidation:

18    $[ISO]_{i,D} = [ISO] \times e^{(k \times [OH] \times \Delta t)}$ (Eq.9)

19    $[ISO]_{i,N} = [ISO] \times e^{(k \times [NO_3] \times \Delta t)}$ (Eq.10)

20   By determining the concentration of radical (*i.e.* OH and NO₃) and atmospheric reaction time of isoprene,

21   the initial isoprene can be calculated.

22   Two issues arise when applying this "back-of-the-envelope" method to the present study (Wolfe et al.,

23   2016). First, the yields from OH-initiated isoprene oxidation are a nonlinear function of nitrogen oxide

24   (NO). Previous applications of this method (de Gouw, 2005;Roberts et al., 2006;Stroud et al., 2001;Karl et

25   al., 2007;Kuhn et al., 2007) have assumed lab-derived high-NO yields of 0.33 and 0.23 for MVK and

26   MACR, respectively (Atkinson and Arey, 2003a), but this may not be appropriate in the present study. Thus

27   we chose the yields derived from the latest Master Chemical Mechanism (MCM) v3.3.1 (Jenkin et al.,

28   2015). The resulting yield curves are interpolated to observed NO mixing ratios (Fig. S7). The yields from

29   NO₃-initiated isoprene oxidation are constants (Table S1). Second, the implied initial isoprene is depended

30   on the mixing ratios of radical and the atmospheric reaction time of isoprene. Thus in this study we

31   introduce the term "exposure" (de Gouw, 2005;Jimenez et al., 2009;Wolfe et al., 2016) defined here as the

product of radical concentration and reaction time ($Exposure = [Radical] \times \Delta t$). Exposures can be obtained by the following two-step process.

First, for any given exposure, a daughter/parent ratio can be expected based on Eq. (5–8), and the theoretical line of [MVK]/[isoprene] versus [MACR]/[isoprene] can be depicted (Stroud et al., 2001;Apel et al., 2002;Roberts et al., 2006;Guo et al., 2012;Wolfe et al., 2016). The range of exposure thus can be derived by comparing the expected daughter/parent ratio with observed data. Then the range of the ratio of initial over observed isoprene (ISO_i/ISO_o) can be calculated based on Eq. (9–10). Fig. S10 compares the relationship of measured data against theoretical trends predicted by the sequential reaction calculation for the daytime and nighttime hours. It can be seen that the observed [MVK]/[isoprene] versus [MACR]/[isoprene] exhibit a tight linear correlation (R^2=0.68 and 0.72 for daytime and nighttime periods, respectively). The measured data fit the predicted line well, although most of the measured data are above the predicted line, which is consistent with some previous studies (Stroud et al., 2001;Apel et al., 2002;Guo et al., 2012). Apart from the uncertainties mentioned in the Section 2.5 of the manuscript, the additional sources of MVK and MACR from isoprene oxidation by daytime NO_3 (Xue et al., 2016) and nighttime OH (Lu et al., 2014) which both were not taken into account in the present study might also be the causes. The theoretical slope agrees well with observations, indicating OH exposures of $0.1-12 \times 10^6$ molecules cm^{-3} h and NO_3 exposures of $4-28 \times 10^8$ molecules cm^{-3} h for daytime and nighttime periods, respectively.

Second, detailed profiles of exposure can be directly calculated from the observed daughter/parent ratios by inverting Eq. (5–8):

$$EXPO_{OH,MVK} = \frac{\ln\left(1 - \frac{[MVK]}{[ISO]} \times \frac{k_{MVK,OH} - k_{ISO,OH}}{y_{MVK,OH}\,k_{ISO,OH}}\right)}{(k_{ISO,OH} - k_{MVK,OH})} \tag{Eq.11}$$

$$EXPO_{OH,MACR} = \frac{\ln\left(1 - \frac{[MACR]}{[ISO]} \times \frac{k_{MACR,OH} - k_{ISO,OH}}{y_{MACR,OH}\,k_{ISO,OH}}\right)}{(k_{ISO,OH} - k_{MACR,OH})} \tag{Eq.12}$$

$$EXPO_{NO_3,MVK} = \frac{\ln\left(1 - \frac{[MVK]}{[ISO]} \times \frac{k_{MVK,NO_3} - k_{ISO,NO_3}}{y_{MVK,NO_3}\,k_{ISO,NO_3}}\right)}{(k_{ISO,NO_3} - k_{MVK,NO_3})} \tag{Eq.13}$$

$$EXPO_{NO_3,MACR} = \frac{\ln\left(1 - \frac{[MACR]}{[ISO]} \times \frac{k_{MACR,NO_3} - k_{ISO,NO_3}}{y_{MACR,NO_3}\,k_{ISO,NO_3}}\right)}{(k_{ISO,NO_3} - k_{MACR,NO_3})} \tag{Eq.14}$$

Where $EXPO_{OH,\ MVK}$, $EXPO_{OH,\ MACR}$, $EXPO_{NO_3,\ MVK}$, and $EXPO_{NO_3,\ MACR}$ represent the derived exposures from [MVK]/[isoprene] and [MACR]/[isoprene] for daytime and nighttime periods.

Calculated daytime OH exposures and nighttime NO_3 exposures range from 1.0×10^5 to 1.3×10^7 molecules cm^{-3} h and 3.5×10^8 to 3.2×10^9 molecules cm^{-3} h, respectively (Fig. S11). The OH and NO_3 exposures derived from two ratios exhibit a good linear correlation (R^2=0.63 and 0.70 for OH and NO_3, respectively), and results derived from [MACR]/[isoprene] are 4% and 18% lower than those from

1 [MVK]/[isoprene] on average, respectively, and we use the mean of these two values. The median and

2 mean OH exposure is 1.9 and 2.5×10^6 molecules cm^{-3} h, respectively. For NO$_3$ exposure, the median and

3 mean value is close (15.8 and 16.2×10^8 molecules cm^{-3} h, respectively).

4 **Text S3. Data processing, graph plotting and graphical source identification by R**

5 In this study, the open source R package "openair" was utilized for data processing and graph plotting

6 (Carslaw and Ropkins, 2012;Carslaw, 2015). Specifically, for those dedicated functions used, the

7 "transform", "selectByDate", "merge" and "subset" functions were used to calculate and filter the data. The

8 "quantile", "summary" and "t.test" functions were used to do statistical analysis. The "timePlot" function

9 was used to plot time series of measured species. The "plot" function was used to plot scatter and diagram

10 diurnal variations. In particular, the "polarPlot" function was used for source identification.

11 The lifetimes of MVK and MACR by OH loss is 1.9 and 1.0 hours, respectively, assuming 12-h daytime

12 OH = 8.0×10^6 molecules cm^{-3} (Table S1). The average daytime wind speed was 3.9 ± 0.2 m s^{-1} at the site,

13 and the distance between the sampling sit and the nearest urban center is 38 km (Fig. S12), the air parcel

14 from upwind locations would spend about 2.7 hours to arrive at the sampling site. This is enough time for

15 the depletion of MVK and MACR along the traveling path during the daytime. However, the nighttime

16 chemical oxidation of MVK and MACR was slow, with lifetimes of MVK and MACR by NO$_3$ oxidation of

17 0.5 years and 72 hours, respectively, assuming 12-h nighttime NO$_3$ = 5.0×10^8 molecules cm^{-3} (Table S1).

18 Apart from biogenic sources, the anthropogenic sources of MVK and MACR, *e.g.* motor vehicles, biomass

19 burning and industrial sources, have been reported by some previous studies (Borbon et al., 2001;Wagner

20 and Kuttler, 2014;Hsieh et al., 2016;Diao et al., 2016). Therefore, the regional transport of MVK- or

21 MACR- laden air could affect the observed nighttime (MVK+MACR)/isoprene ratios at the site.

22 Hence, the "polarPlot" technique was used for source identification in this study. In "polarPlot" drawing,

23 the species concentrations are shown to vary by wind speed and wind direction, and plots are shown as a

24 continuous surface, and the surfaces are calculated through modeling using smoothing techniques. These

25 plots have been proved to be useful for the quick gaining of a graphical impression of potential sources'

26 influences at a location in recent publications that describe or use the technique (Valach et al., 2014;Chang

27 et al., 2017). Fig. S13 shows the polarplots of isoprene, MVK and MACR during the study. During the

28 sampling periods, the air masses reaching the site were mainly from the southwest and northeast directions.

29 The red dotted sectorial domains are interpreted as the regional transport interference as the concentrations

30 of species increase with increasing wind speed. The high levels of species at high wind speeds most likely

31 came from the nearby urban centers. Therefore, measurements that are deemed to be affected by regional

32 transport are all excluded from the dataset in the analysis.

References

Apel, E. C., Riemer, D. D., Hills, A., Baugh, W., Orlando, J., Faloona, I., Tan, D., Brune, W., Lamb, B., Westberg, H., Carroll, M. A., Thornberry, T., and Geron, C. D.: Measurement and interpretation of isoprene fluxes and isoprene, methacrolein, and methyl vinyl ketone mixing ratios at the PROPHET site during the 1998 Intensive, Journal of Geophysical Research-Atmospheres, 107, 15, 10.1029/2000jd000225, 2002.

Atkinson, R., and Arey, J.: Gas-phase tropospheric chemistry of biogenic volatile organic compounds: a review, Atmos Environ, 37, S197-S219, 10.1016/S1352-2310(03)00391-1, 2003a.

Atkinson, R., and Arey, J.: Atmospheric degradation of volatile organic compounds, Chem Rev, 103, 4605-4638, 10.1021/cr0206420, 2003b.

Atkinson, R., Baulch, D. L., Cox, R. A., and Crowley, J. N.: Evaluated kinetic and photochemical data for atmospheric chemistry: Volume II – gas phase reactions of organic species, Atmospheric Chemistry and Physics (ACP) & Discussions (ACPD), 2006.

Borbon, A., Fontaine, H., Veillerot, M., Locoge, N., Galloo, J. C., and Guillermo, R.: An investigation into the traffic-related fraction of isoprene at an urban location, Atmos Environ, 35, 3749-3760, Doi 10.1016/S1352-2310(01)00170-4, 2001.

Carslaw, D. C., and Ropkins, K.: openair - An R package for air quality data analysis, Environmental Modelling & Software, 27-28, 52-61, 10.1016/j.envsoft.2011.09.008, 2012.

Chang, Y., Huang, K., Deng, C., Zou, Z., Liu, S., and Zhang, Y.: First long-term and near real-time measurement of atmospheric trace elements in Shanghai, China, Atmospheric Chemistry and Physics Discussions, 1-49, 10.5194/acp-2017-613, 2017.

de Gouw, J. A.: Budget of organic carbon in a polluted atmosphere: Results from the New England Air Quality Study in 2002, Journal of Geophysical Research, 110, 22, 10.1029/2004jd005623, 2005.

Diao, L. J., Choi, Y., Czader, B., Li, X. S., Pan, S., Roy, A., Souri, A. H., Estes, M., and Jeon, W.: Discrepancies between modelled and observed nocturnal isoprene in an urban environment and the possible causes: A case study in Houston, Atmos Res, 181, 257-264, 10.1016/j.atmosres.2016.07.009, 2016.

Guo, H., Ling, Z. H., Simpson, I. J., Blake, D. R., and Wang, D. W.: Observations of isoprene, methacrolein (MAC) and methyl vinyl ketone (MVK) at a mountain site in Hong Kong, Journal of Geophysical Research-Atmospheres, 117, 13, 10.1029/2012jd017750, 2012.

Hsieh, H., Ouyang, C., and Wang, J.: Revelation of Coupling Biogenic with Anthropogenic Isoprene by Highly Time-Resolved Observations, Aerosol and Air Quality Research, 10.4209/aaqr.2016.04.0133, 2016.

Jenkin, M. E., Young, J. C., and Rickard, A. R.: The MCM v3.3.1 degradation scheme for isoprene, Atmos Chem Phys, 15, 11433-11459, 10.5194/acp-15-11433-2015, 2015.

Jimenez, J. L., Canagaratna, M. R., Donahue, N. M., Prevot, A. S., Zhang, Q., Kroll, J. H., DeCarlo, P. F., Allan, J. D., Coe, H., Ng, N. L., Aiken, A. C., Docherty, K. S., Ulbrich, I. M., Grieshop, A. P., Robinson, A. L., Duplissy, J., Smith, J. D., Wilson, K. R., Lanz, V. A., Hueglin, C., Sun, Y. L., Tian, J., Laaksonen, A., Raatikainen, T., Rautiainen, J., Vaattovaara, P., Ehn, M., Kulmala, M., Tomlinson, J. M., Collins, D. R., Cubison, M. J., Dunlea, E. J., Huffman, J. A., Onasch, T. B., Alfarra, M. R., Williams, P. I., Bower, K., Kondo, Y., Schneider, J., Drewnick, F., Borrmann, S., Weimer, S., Demerjian, K., Salcedo, D., Cottrell, L., Griffin, R., Takami, A., Miyoshi, T., Hatakeyama, S., Shimono, A., Sun, J. Y., Zhang, Y. M., Dzepina, K., Kimmel, J. R., Sueper, D., Jayne, J. T., Herndon, S. C., Trimborn, A. M., Williams, L. R., Wood, E. C., Middlebrook, A. M., Kolb, C. E., Baltensperger, U., and Worsnop, D. R.: Evolution of organic aerosols in the atmosphere, Science, 326, 1525-1529, 10.1126/science.1180353, 2009.

Karl, T., Guenther, A., Yokelson, R. J., Greenberg, J., Potosnak, M., Blake, D. R., and Artaxo, P.: The tropical forest and fire emissions experiment: Emission, chemistry, and transport of biogenic volatile organic compounds in the lower atmosphere over Amazonia, Journal of Geophysical Research-Atmospheres, 112, 17, 10.1029/2007jd008539, 2007.

Kuhn, U., Andreae, M. O., Ammann, C., Araujo, A. C., Brancaleoni, E., Ciccioli, P., Dindorf, T., Frattoni, M., Gatti, L. V., Ganzeveld, L., Kruijt, B., Lelieveld, J., Lloyd, J., Meixner, F. X., Nobre, A. D., Poschl, U., Spirig, C., Stefani, P., Thielmann, A., Valentini, R., and Kesselmeier, J.: Isoprene and monoterpene fluxes from Central Amazonian rainforest inferred from tower-based and airborne measurements, and implications on the atmospheric chemistry and the local carbon budget, Atmos Chem Phys, 7, 2855-2879, 10.5194/acp-7-2855-2007, 2007.

Lu, K. D., Rohrer, F., Holland, F., Fuchs, H., Brauers, T., Oebel, A., Dlugi, R., Hu, M., Li, X., Lou, S. R., Shao, M., Zhu, T., Wahner, A., Zhang, Y. H., and Hofzumahaus, A.: Nighttime observation and chemistry of HOx in the Pearl River Delta and Beijing in summer 2006, Atmos Chem Phys, 14, 4979-4999, 10.5194/acp-14-4979-2014, 2014.

Parrish, D. D., Stohl, A., Forster, C., Atlas, E. L., Blake, D. R., Goldan, P. D., Kuster, W. C., and de Gouw, J. A.: Effects of mixing on evolution of hydrocarbon ratios in the troposphere, Journal of Geophysical Research-Atmospheres, 112, 10.1029/2006jd007583, 2007.

Roberts, J. M., Marchewka, M., Bertman, S. B., Goldan, P., Kuster, W., de Gouw, J., Warneke, C., Williams, E., Lerner, B., Murphy, P., Apel, E., and Fehsenfeld, F. C.: Analysis of the isoprene chemistry observed during the New England Air Quality Study (NEAQS) 2002 intensive experiment, Journal of Geophysical Research-Atmospheres, 111, 10.1029/2006jd007570, 2006.

Shiu, C. J., Liu, S. C., Chang, C. C., Chen, J. P., Chou, C. C. K., Lin, C. Y., and Young, C. Y.: Photochemical production of ozone and control strategy for Southern Taiwan, Atmos Environ, 41, 9324-9340, 10.1016/j.atmosenv.2007.09.014, 2007.

Stroud, C. A., Roberts, J. M., Goldan, P. D., Kuster, W. C., Murphy, P. C., Williams, E. J., Hereid, D., Parrish, D., Sueper, D., Trainer, M., Fehsenfeld, F. C., Apel, E. C., Riemer, D., Wert, B., Henry, B., Fried, A., Martinez-Harder, M., Harder, H., Brune, W. H., Li, G., Xie, H., and Young, V. L.: Isoprene and its oxidation products, methacrolein and methylvinyl ketone, at an urban forested site during the 1999 Southern Oxidants Study, Journal of Geophysical Research-Atmospheres, 106, 8035-8046, Doi 10.1029/2000jd900628, 2001.

Valach, A. C., Langford, B., Nemitz, E., MacKenzie, A. R., and Hewitt, C. N.: Concentrations of selected volatile organic compounds at kerbside and background sites in central London, Atmos Environ, 95, 456-467, 10.1016/j.atmosenv.2014.06.052, 2014.

Wagner, P., and Kuttler, W.: Biogenic and anthropogenic isoprene in the near-surface urban atmosphere — A case study in Essen, Germany, Science of The Total Environment, 475, 104-115, http://dx.doi.org/10.1016/j.scitotenv.2013.12.026, 2014.

Wolfe, G. M., Kaiser, J., Hanisco, T. F., Keutsch, F. N., de Gouw, J. A., Gilman, J. B., Graus, M., Hatch, C. D., Holloway, J., Horowitz, L. W., Lee, B. H., Lerner, B. M., Lopez-Hilifiker, F., Mao, J., Marvin, M. R., Peischl, J., Pollack, I. B., Roberts, J. M., Ryerson, T. B., Thornton, J. A., Veres, P. R., and Warneke, C.: Formaldehyde production from isoprene oxidation across NOx regimes, Atmos Chem Phys, 16, 2597-2610, 10.5194/acp-16-2597-2016, 2016.

Xu, Z., Wang, T., Xue, L. K., Louie, P. K. K., Luk, C. W. Y., Gao, J., Wang, S. L., Chai, F. H., and Wang, W. X.: Evaluating the uncertainties of thermal catalytic conversion in measuring atmospheric nitrogen dioxide at four differently polluted sites in China, Atmos Environ, 76, 221-226, 10.1016/j.atmosenv.2012.09.043, 2013.

Xue, L. K., Gu, R. R., Wang, T., Wang, X. F., Saunders, S., Blake, D., Louie, P. K. K., Luk, C. W. Y., Simpson, I., Xu, Z., Wang, Z., Gao, Y., Lee, S. C., Mellouki, A., and Wang, W. X.: Oxidative capacity and radical chemistry in the polluted atmosphere of Hong Kong and Pearl River Delta region: analysis of a severe photochemical smog episode, Atmos Chem Phys, 16, 9891-9903, 10.5194/acp-16-9891-2016, 2016.

1 Zha, Q.: Measurement of nitrous acid (HONO) and the implications to photochemical pollution, MPhil dissertation, Department
2 of Civil and Environmental Engineering, The Hong Kong Polytechnic University, 2015.

Tables

Table S1. Rate constants and lifetime for isoprene, MVK and MACR, and yields of MVK and MACR from the isoprene reactions.

Compound	Rate constants [a] with			Yield [b] from isoprene reaction with / (lifetime [b] due to)		
	OH	NO_3	O_3	OH	NO_3	O_3
Isoprene	1.0×10^{-10}	7.0×10^{-13}	1.3×10^{-17}	- / 0.4 h	- / 0.8 h	- / 24 h
MVK	2.0×10^{-11}	3.2×10^{-16}	5.2×10^{-18}	0.33 / 1.9 h	0.035 / 0.5 yr	0.16 / 61 h
MACR	2.9×10^{-11}	3.7×10^{-15}	1.2×10^{-18}	0.23 / 1.0 h	0.035 / 72 h	0.41 / 10 d
Benzene	1.2×10^{-12}	$<3.0\times10^{-17}$	$<1.0\times10^{-21}$	- / 9.5 d [c]	- / >4 yr	- / >4.5 yr
Toluene	5.6×10^{-12}	7.8×10^{-17}	$<1.0\times10^{-21}$	- / 2.1 d [c]	- / 1.8 yr	- / >4.5 yr
Ethylbenzene	7.0×10^{-12}	$<6.0\times10^{-16}$	$<1.0\times10^{-21}$	- / 1.7 d [c]	-	-
m,p-Xylene	1.9×10^{-11}	3.8×10^{-16}	$<1.0\times10^{-21}$	- / 0.6 d [c]	- / 0.5 yr	- / >5 yr

6 [a] The 298 K rate constants (unit in $cm^3 \, molecule^{-1} \, s^{-1}$) are taken from Atkinson and Arey (2003b), Atkinson et al. (2006) and
7 IUPAC database (http://iupac.pole-ether.fr/).
8 [b] (Atkinson and Arey, 2003a, b) and references therein. Lifetime calculated at 298 K using the following: for OH radical
9 reactions, a 12-h daytime average of 8.0×10^6 molecules cm^{-3}; for NO_3 radical reactions, a 12-h nighttime average of 5.0×10^8
10 molecules cm^{-3}; and for O_3, a 24-h average of 1.0×10^{12} molecules cm^{-3}.
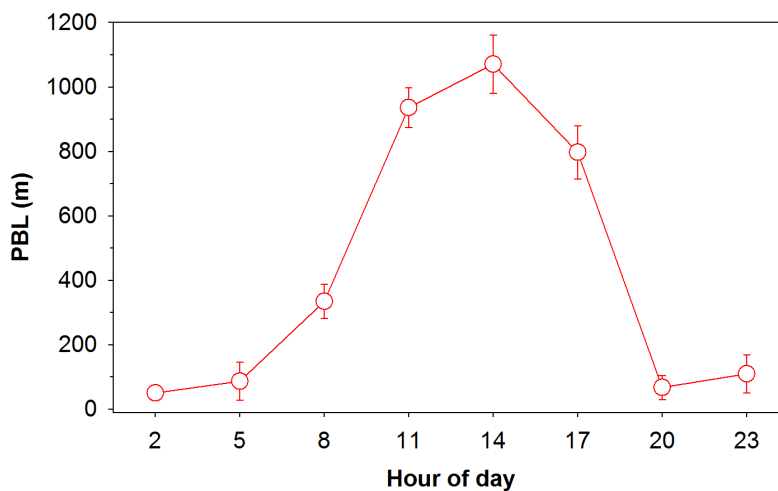11 [c] For a 12-h daytime average OH radical concentration of 2.0×10^6 molecules cm^{-3}.
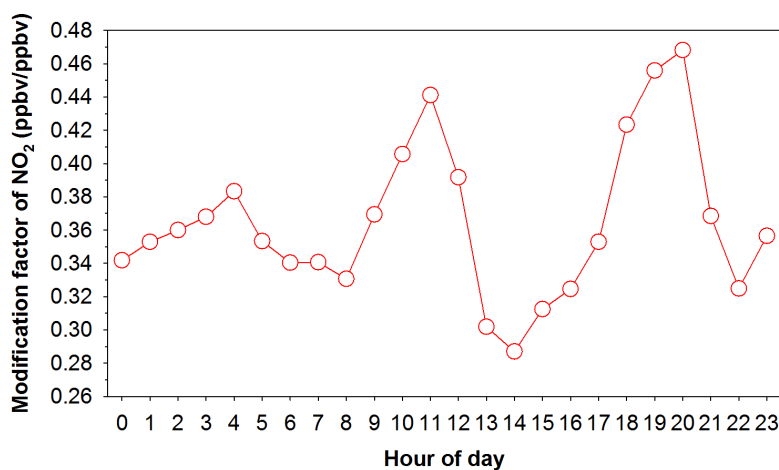
Figures


Fig. S1: Hourly modification factor of NO_2 during Jul 15 – Aug 17 2016 at the Nanling site. The data in the figure are reproduced from the study conducted at a high-altitude mountain site (Mt. Tai) in central-eastern China by Xu et al. (2013).

1
2 **Fig. S2:** Diurnal variation of the Planetary Boundary Layer (PBL) height (data provided by Real-time
3 Environmental Applications and Display System, https://ready.arl.noaa.gov/READYamet.php, unit in m) at Nanling
4 site (1,690 m a.s.l.) during Jul 15–Aug 17 2016. Error bars indicate the 95% confidence interval.
5
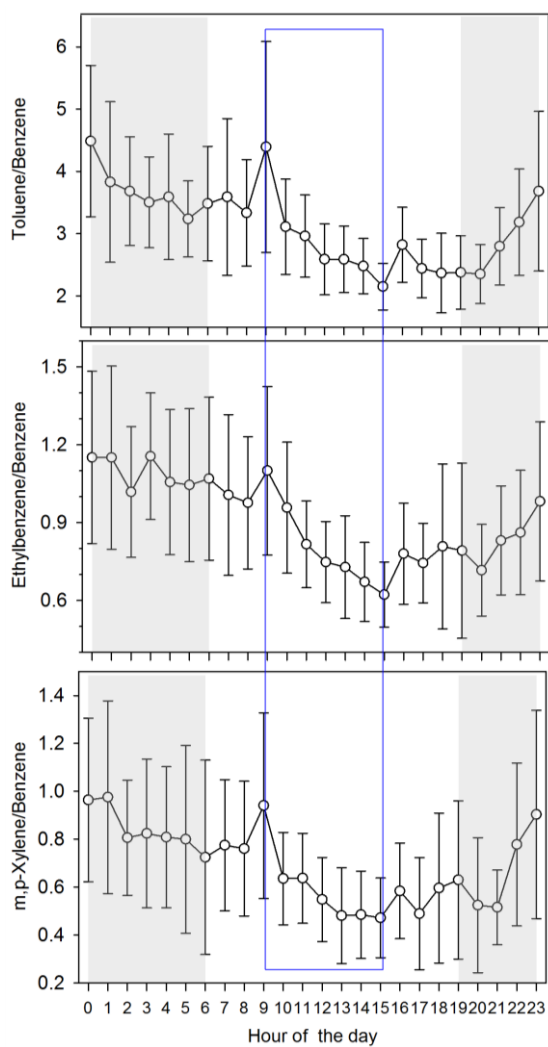
6

7 **Fig. S3:** Diurnal variations of toluene/benzene, ethylbenzene/benzene and m,p-xylene/benzene ratios at Nanling site
8 during Jul 15–Aug 17 2016. Shaded regions denote the nighttime periods. Error bars indicate the 95% confidence
9 interval. Blue boxed area denotes periods for the calculating of regional mixing ratios of daytime OH.

9
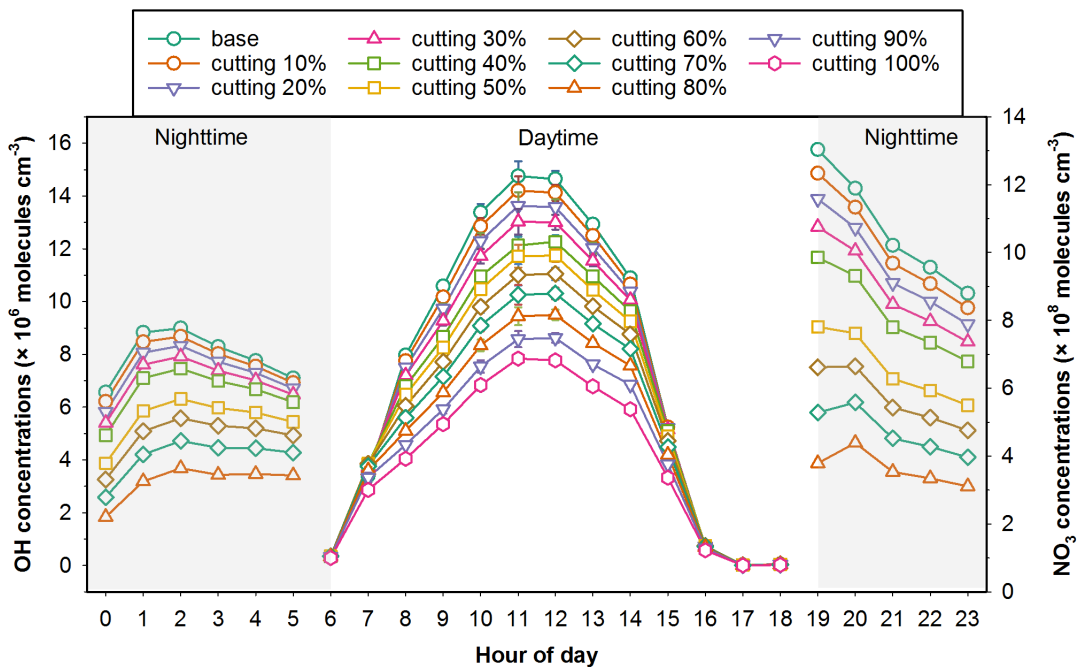
1
2 **Fig. S4:** Sensitivity analysis of PBM-MCM modelled daytime OH and nighttime NO_3 with reduced NO_2

3 concentrations for the period Aug 11 − Aug 15 2016.

4
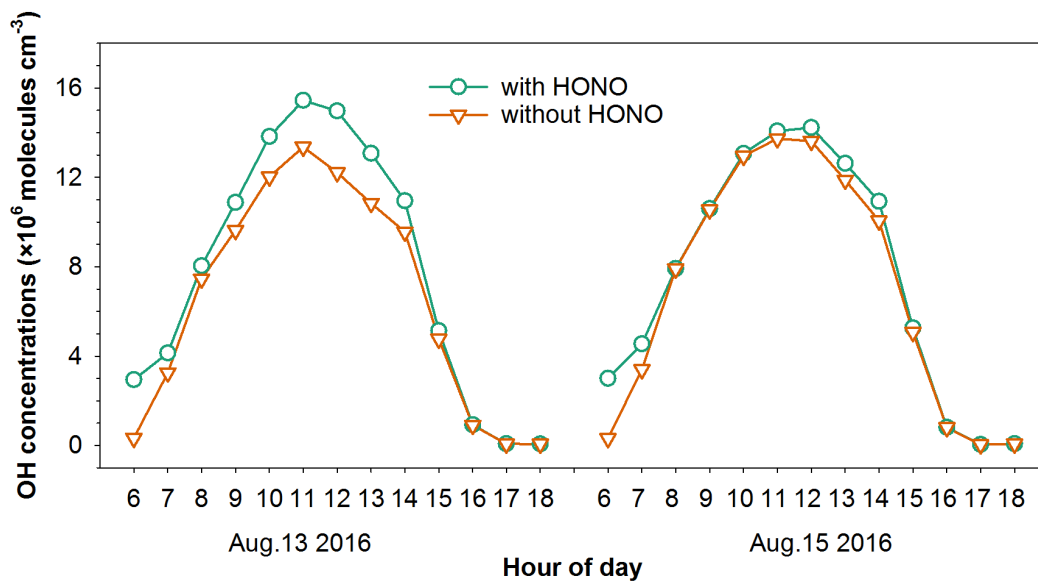
5

6 **Fig. S5:** Sensitivity analysis of PBM-MCM modelled daytime OH with and without HONO for the period Aug 13

7 and Aug 15 2016. The HONO data was obtained from the study conducted at a background site (Hok Tsui) in Hong

8 Kong in autumn 2012 by Zha (2015).

9

1
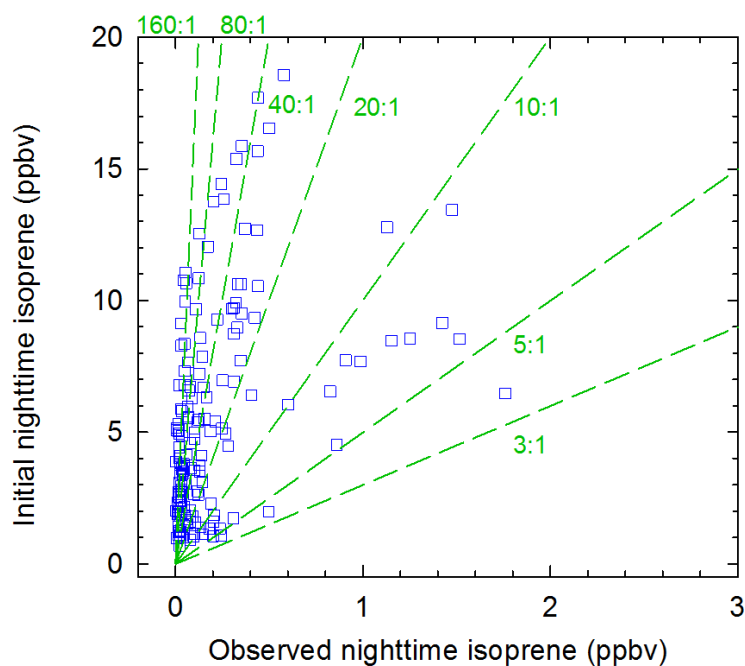
Fig. S6: Comparison of observed and initial isoprene mixing ratios at night. Green dashed lines denote slopes for different ratios of initial to observed isoprene.

4

5
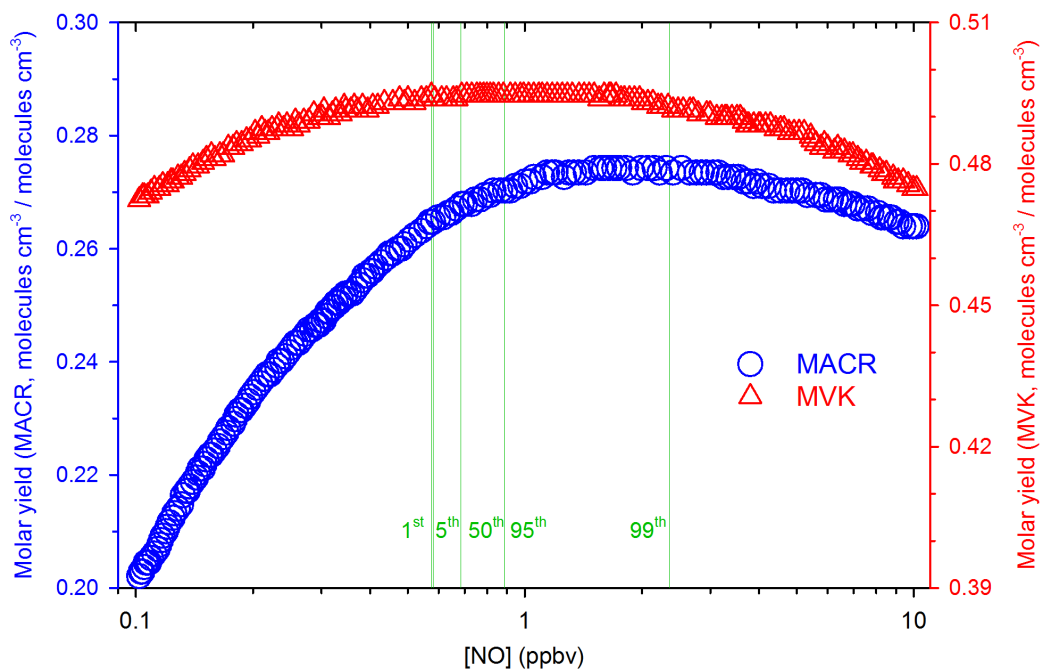
Fig. S7: Molar yields of the main first-generation products (MVK and MACR) of the OH-initiated oxidation of isoprene as a function of NO mixing ratio, at 298 K, as represented in MCM v3.3.1 (Jenkin et al., 2015). Thin green vertical lines denote, from left to right, the 1st, 5th, 50th, 95th and 99th percentiles of hourly NO observed during the present study.
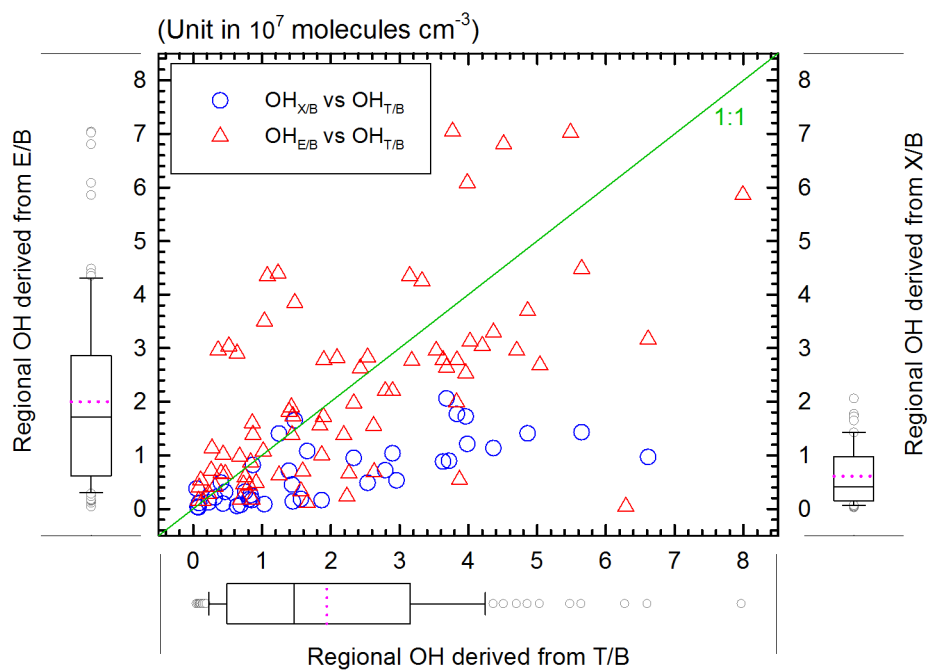
Fig. S8: Scatterplots of the regional mixing ratios of OH during 09:00 – 15:00 LST derived from the toluene/benzene ($OH_{T/B}$), ethylbenzene/benzene ($OH_{E/B}$) and m,p-xylene/benzene ($OH_{X/B}$) ratios. The green line denotes a 1:1 relationship. Next to axes are the box and whisker plots of each result, and the pink dotted lines denote the mean values.
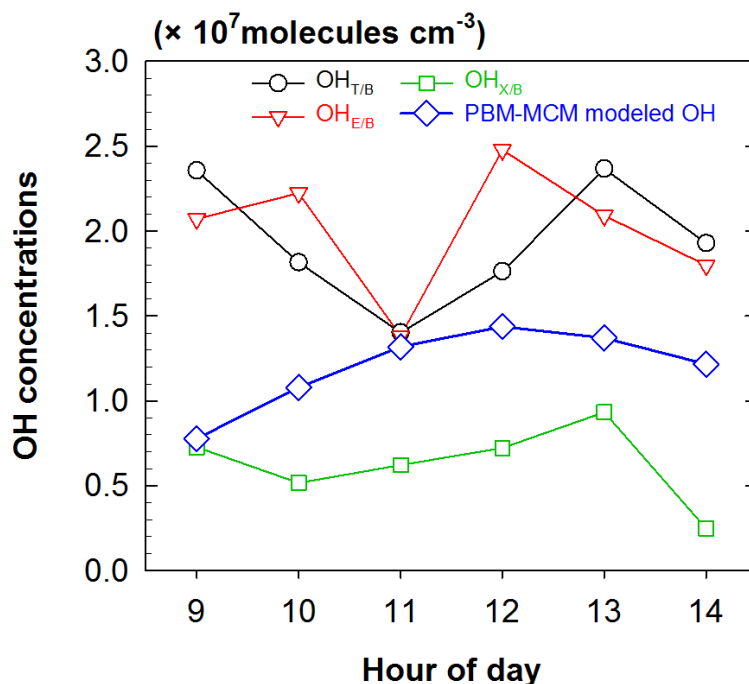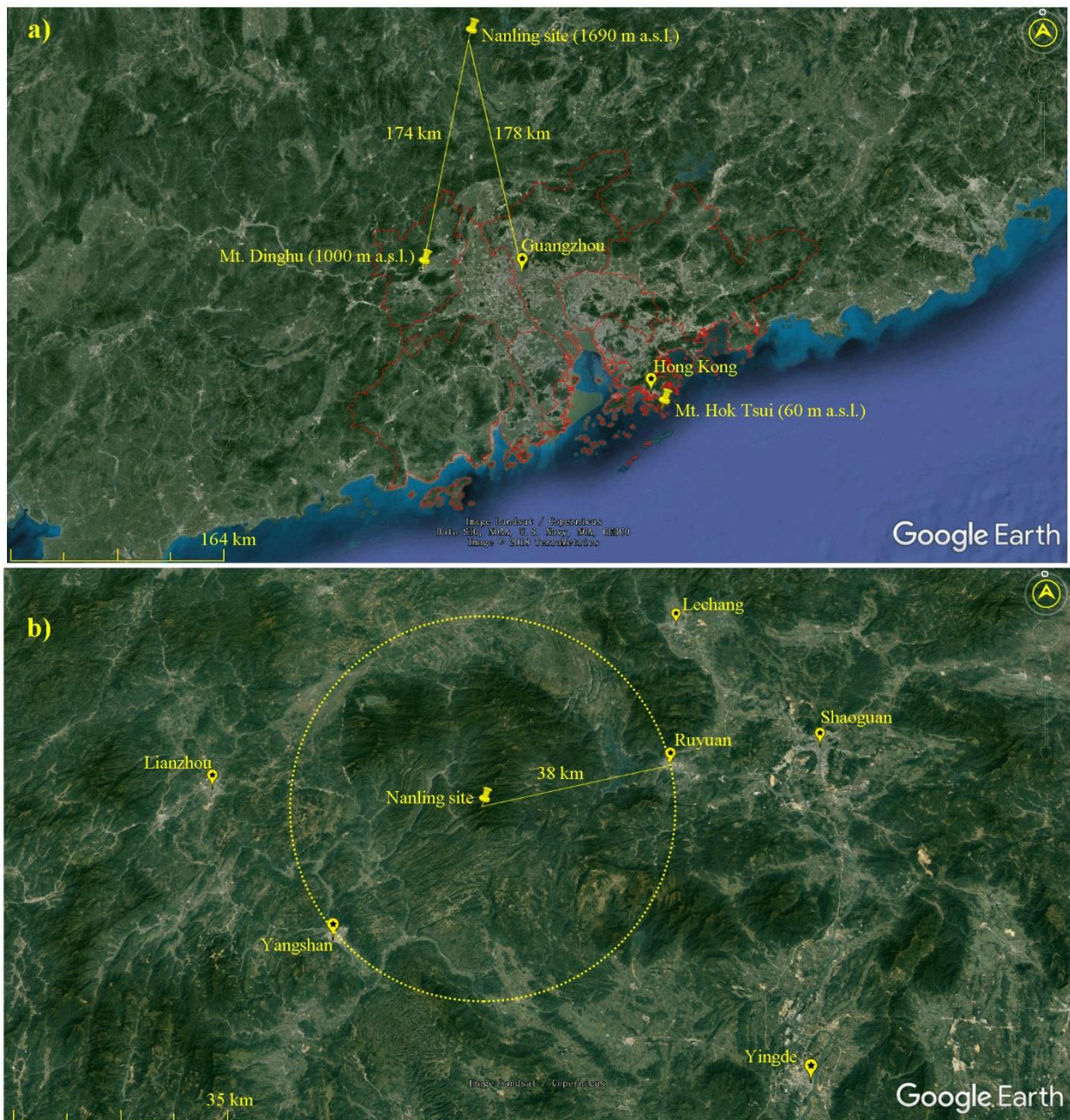

Fig. S9: Average hourly variations of the regional concentrations of OH derived from the toluene/benzene ratio ($OH_{T/B}$), ethylbenzene/benzene ratio ($OH_{E/B}$) and m,p-xylene/benzene ratio ($OH_{X/B}$) and the site-level OH modelled by PBM-MCM between 09:00 and 15:00 LST.
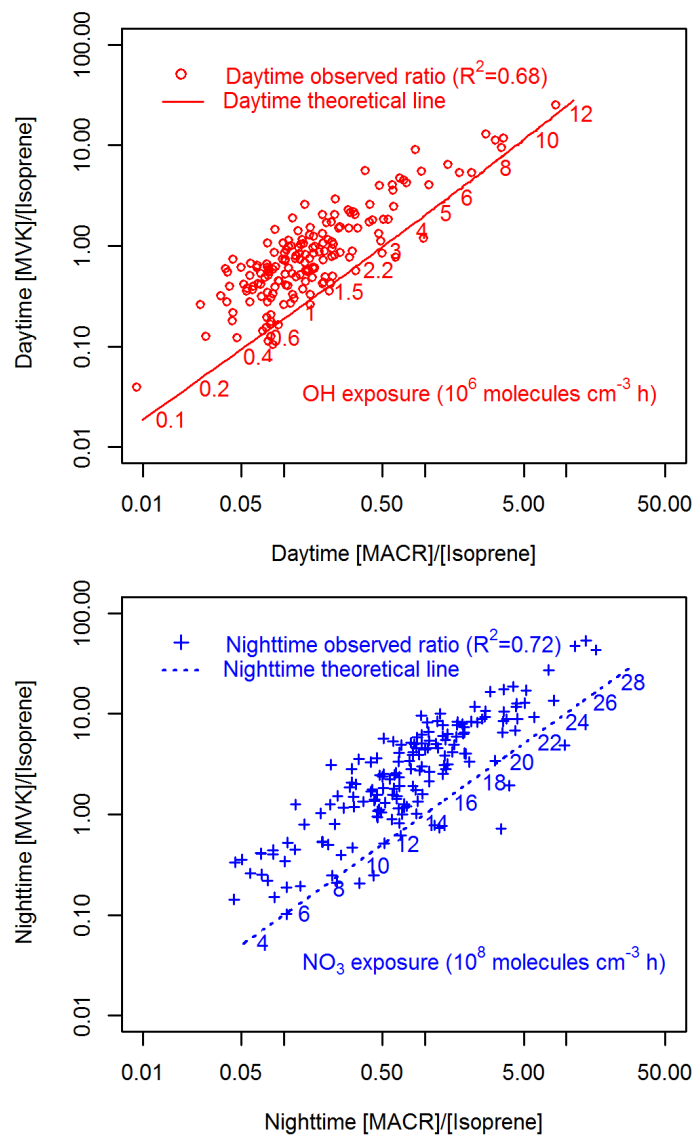
Fig. S10: Ranges of exposure derived by the progression of product/parent ratios (*i.e.* [MVK]/[isoprene] and [MACR]/[isoprene], unit: molecules cm^{-3} / molecules cm^{-3}). Red circles and blue crosses show the observed ratios for the daytime and nighttime measurements, respectively. The red solid and blue dashed lines are the theoretical product/parent ratios of isoprene sequential reaction scheme calculation. The numbers next to the line indicate the theoretical exposures (the product of radical concentration and reaction time) corresponding to any given product –parent relationship.

Fig. S11: Scatter plots of exposures derived from observed [MVK]/[isoprene] versus that from [MACR]/[isoprene]. The unit of OH exposure and NO_3 exposure is 10^6 molecules cm^{-3} h and 10^8 molecules cm^{-3} h, respectively.

Fig. S12: (a) Location of the Nanling site, Dinghu Mountain site, Hok Tsui site, Guangzhou and Hong Kong. The Nanling site is 174 km northeast to the Dinghu Mountain site and 178 km northwest to Guangzhou. Red outlined domain represent the Pearl River Delta region. (b) Map showing the nearest urban centers (Yangshan County, Ruyuan County, Lechang City, Lianzhou City, Shaoguan City and Yingde City) around the site.
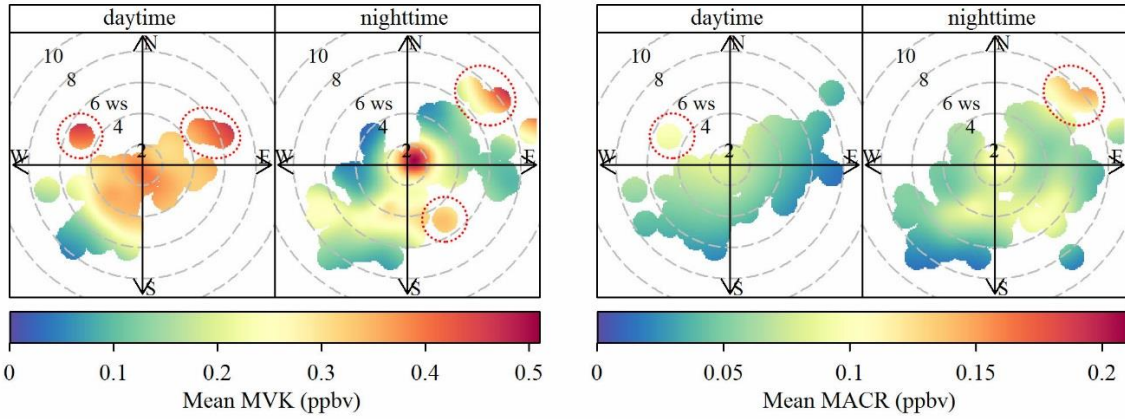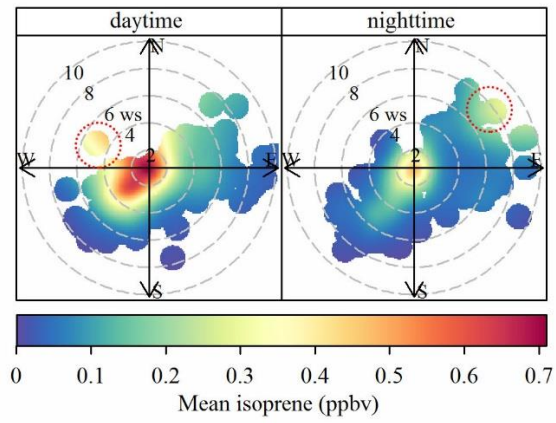
Fig. S13: Daytime and nighttime polarplots of isoprene, MVK and MACR during the sampling period (Jul 15–Aug 17 2016). Concentrations varied by wind speed (ws, unit in m/s) and wind direction. Red dotted sectorial domains represent the interferences of regional transport from nearby urban centres.